Journal of
Composites Science

MDPI

Review

Recent Advances on The Applications of Phase Change Materials in Cold Thermal Energy Storage: A Critical Review

Farhan Lafta Rashid [1], Mudhar A. Al-Obaidi [2,3], Anmar Dulaimi [4,5], Luís Filipe Almeida Bernardo [6,*], Zeina Ali Abdul Redha [7], Hisham A. Hoshi [8], Hameed B. Mahood [4,9] and Ahmed Hashim [10]

1 Petroleum Engineering Department, College of Engineering, University of Kerbala, Karbala 56001, Iraq; farhan.lefta@uokerbala.edu.iq
2 Technical Instructor Training Institute, Middle Technical University, Baghdad 10074, Iraq; dr.mudhar.alaubedy@mtu.edu.iq
3 Technical Institute of Baquba, Middle Technical University, Baquba 32001, Iraq
4 College of Engineering, University of Warith Al-Anbiyaa, Karbala 56001, Iraq; a.f.dulaimi@uowa.edu.iq or a.f.dulaimi@ljmu.ac.uk (A.D.); h.al-muhammedawi@bham.ac.uk (H.B.M.)
5 School of Civil Engineering and Built Environment, Liverpool John Moores University, Liverpool L3 2ET, UK
6 Department of Civil Engineering and Architecture, University of Beira Interior, 6201-001 Covilhã, Portugal
7 Energy Engineering Department, University of Baghdad, Baghdad 10011, Iraq; dr.zeina.a@coeng.uobaghdad.edu.iq
8 Electromechanical Engineering Department, University of Technology, Baghdad 10066, Iraq; 50254@uotechnology.edu.iq
9 Centre of Sustainable Cooling, School of Chemical Engineering, University of Birmingham, Birmingham B15 2TT, UK
10 Department of Physics, College of Education for Pure Sciences, University of Babylon, Babylon 51002, Iraq; ahmed_taay@yahoo.com
* Correspondence: lfb@ubi.pt

Abstract: Cold thermal energy storage (CTES) based on phase change materials (PCMs) has shown great promise in numerous energy-related applications. Due to its high energy storage density, CTES is able to balance the existing energy supply and demand imbalance. Given the rapidly growing demand for cold energy, the storage of hot and cold energy is emerging as a particularly attractive option. The main purpose of this study is to provide a comprehensive overview of the current research progress on the utilisation of PCMs in CTES. The greatest difficulties associated with using PCMs for CTES are also examined in this overview. In this regard, a critical evaluation of experimental and numerical studies of the heat transfer properties of various fundamental fluids using PCMs is conducted. Specifically, several aspects that affect the thermal conductivity of PCMs are investigated. These factors include nanoparticle-rich PCM, a form of encapsulated PCM, solids volume percentage, and particle size. Discussions focus on observations and conclusions are drawn from conducted studies on PCMs used in CTES. Based on the findings of this study, a set of plausible recommendations are made for future research initiatives.

Keywords: cold thermal energy storage (CTES); phase change materials (PCMs); heat transfer; cold applications; review

Citation: Rashid, F.L.; Al-Obaidi, M.A.; Dulaimi, A.; Bernardo, L.F.A.; Redha, Z.A.A.; Hoshi, H.A.; Mahood, H.B.; Hashim, A. Recent Advances on The Applications of Phase Change Materials in Cold Thermal Energy Storage: A Critical Review. *J. Compos. Sci.* **2023**, *7*, 338. https://doi.org/10.3390/jcs7080338

Academic Editors: Francesco Tornabene and Farooq Sher

Received: 8 July 2023
Revised: 10 August 2023
Accepted: 16 August 2023
Published: 18 August 2023

1. Introduction

Fossil fuels are an important source of energy worldwide, accounting for 85.5% of total energy consumption. However, if humanity continues to use fossil fuels at this consumption level, a range of environmental problems will arise including shifting weather patterns and global temperature increases [1]. Therefore, with the development of energy-saving technologies, the use of new energy and renewable energy has become the focus of global attention. The energy supplied during the day and night varies greatly, which is detrimental to the reliability of the energy transfer system [2]. The most pressing issue

is how to utilise the excess electricity generated at night during the day so that no stress builds up. Refrigeration equipment is one of the remedies to this issue and has developed into a crucial component of reducing the effect of the current crisis on the world's electricity supply due to its distinctive influence on load shifting. Energy storage technology not only speeds up the uptake of new and renewable energy sources but also works well to correct the disparity between supply and demand in the market [3].

To find a solution to this problem, the intelligent use of thermal energy storage (TES) is essential. The technology behind TES has been extensively studied [4,5] and can be classified into three distinct thermal categories: chemical heat, latent heat, and sensible heat. Sensitive heat is the most common form of heat. Besides sensible heat and chemical heat, another way to efficiently utilise energy is to focus on the latent heat generated by phase change materials (PCMs) [6,7]. The phase transition process caused by changes in ambient temperature employs the latent heat method to store and release thermal energy. Constant temperature can be maintained by isothermal absorption and release of heat; this enables efficient use of energy in space and time [8–11]. PCMs are widely used in a wide range of energy conversion fields such as waste heat recovery, Li-ion batteries, building insulation, and solar energy storage [12–23].

The most familiar types of PCMs are eutectic and organic and inorganic. The term "eutectic PCM" refers to mixtures of two or more substances (organic and inorganic PCMs) that, when mixed in a particular proportion, have a lower melting point than any of the constituent parts. They experience a rapid and distinct phase transition while maintaining a steady temperature and releasing or absorbing thermal energy. Moreover, eutectic PCMs can be made so as to generate favourable properties such as a lower melting point or a specific phase change temperature. Salt hydrates, such as calcium chloride and sodium sulphate, are typical examples of eutectic PCMs [24]. Organic PCMs are single-component materials made from organic chemicals or hydrocarbons. Compared to eutectic PCMs, they may display a wider melting temperature range, but they have distinct phase change temperatures. Examples of organic PCMs frequently utilised for cold thermal energy storage include paraffin waxes and fatty acids [25]. Furthermore, solid inorganic phase change materials exhibit elevated latent heat values and high melting temperatures, resulting in effective energy storage and release during phase changes [26]. In this regard, PCMs have been successfully used in different sectors of CTES. The following demonstrates a number of studies encountered during the evaluation of PCMs in CTES.

Veerakumar and Sreekumar (2015) [27] provided a detailed assessment of current breakthroughs and previous research projects using PCMs for cold thermal energy storage. These commercially available PCMs are classified and listed according to their melting point and latent heat of fusion. These PCMs have the potential to be utilised as materials for storing cold energy. Furthermore, methods to improve the thermo-physical properties of PCMs, including encapsulation, increased heat transfer, incorporation of nanostructures, and shape stability, were analysed and discussed in this paper. Corrosion of building materials was also found to affect the stability of the structure.

Nie et al. (2020) [28] revised TES for cold energy storage, focusing on a variety of cryogenic liquid–solid PCMs. A basic overview of the PCM classification system was presented. Recent technologies used to improve PCM performance, in particular their low thermal conductivity, liquid PCM leakage, and limiting their use in TES refrigeration applications with high degrees of sub-cooling, were intensively discussed in this study. Several strategies for improving thermal performance were compared, such as using composite PCMs and massive networks. The application of modelling and experimental research in the field of refrigeration was also highlighted. A number of applications for cold energy storage currently in use have been outlined such as air conditioning and free cooling.

Selvnes et al. (2021) [29] provided a comprehensive overview of recent advances and research surveys on CTES using PCMs in refrigeration systems. They focused on the latest developments in the field. The study included the classification of many types of

PCMs used in a wide set of applications ranging from air conditioning (AC) (20 °C) to food freezing (below −60 °C). Besides providing a list of PCMs currently on the market that operate between 10 °C and −65 °C, the authors provided an indication of the thermophysical characteristics of PCMs that may affect the behaviour and related approaches to characterise PCMs.

Radouane (2022) [30] focused on discussing the fabrication methods of PCMs including encapsulation, hybrid confinement, and polymerization in addition to addressing the enhancement of the thermal conductivity of composite PCMs. The author illustrated the successful utilisation of PCMs in different sectors of energy storage, energy conversion, and thermal management.

Despite the existence of the above attempts to evaluate the contribution of PCMs in the field of CTES, we think that a presentation with a critical assessment of the most recent innovations of utilising PCMs in different applications of CTES has not been conducted in one package yet. Thus, this study intends to fill this gap in the literature by revising the most relevant challenges of deploying PCMs in CTES and then overviewing the most successful associated studies between 2017 and 2022. The covered studies are categorized into experimental, numerical, and experimental and numerical classes. As a direct result, this study intends to discuss the recent advances in the implications of PCMs in different sectors of CTES including buildings, air conditioning and refrigeration, food storage, cold chain applications, and other associated applications. A thorough understanding of the issues in question is necessary to make future progress in the field and to provide actionable answers to questions that arise in many different contexts. Researchers will benefit from this study by gaining a better understanding of the various improvements in PCMs in cold thermal energy storage that still have room for improvement. The recommendations of this study may guide other investigations in the future.

2. Conceptual Challenges of Using PCMs in Different Applications of CTES

Because of their capacity to store and release energy during phase transitions, PCMs have demonstrated significant potential in a variety of CTES applications. However, their use encounters conceptual difficulties that must be overcome in order to maximise usefulness and efficiency. Some of the most significant conceptual issues are as follows [31–35]:

- It is critical to select the appropriate PCM for a given application. PCMs are classified as organic, inorganic, or eutectic mixes, with varying melting and freezing points and latent heat capacities. Choosing a PCM that meets the temperature demands of the application while preserving stability and reliability might be difficult;
- To minimise corrosion problems in low-temperature applications, the construction materials of the container used to hold diverse eutectic PCMs for thermal energy storage must be considered;
- To minimise leakage and assure compatibility with current equipment, PCMs are often enclosed within containers. Finding acceptable encapsulating materials that are PCM-compatible, thermally conductive, and chemically stable might be difficult. Furthermore, the encapsulation technique should not interfere with heat transfer during phase change;
- The rate of heat transmission during the charging (melting) and discharging (solidification) processes determines the effectiveness of PCM-based thermal storage devices. PCMs have a lower and poor thermal conductivity than traditional materials such as metals. This might result in poorer heat transfer rates and might require the use of higher thermal conductivity structures or composites, complicating the process of design and production even more. In this regard, high heat transfer rates can be difficult to achieve, particularly for large-scale applications, because they may necessitate sophisticated heat exchanger designs and adequate interaction with current systems;
- During phase transitions, some PCMs experience considerable volume changes, which can cause mechanical stress and distortion of the incarceration structures. Controlling

these volume variations in order to prevent system damage across several phase change cycles necessitates careful design and research;
- During their lifetime, PCMs are predicted to go through several phase change cycles. A crucial problem is guaranteeing the PCM's stability and strength across many cycles without a substantial drop in effectiveness.

Overcoming these conceptual issues would necessitate collaborative efforts from material scientists, engineers, thermodynamics experts, and system designers. Solving these obstacles will result in enhanced effectiveness and broader adoption of phase change materials in cold thermal energy storage applications.

3. Applications of PCM-Based CTES and Imperative Improvements

The improvement of energy systems that use cold thermal energy requires CTES. Peak load shifting is one of the most often utilised CTES applications. The cold thermal energy produced at nighttime could be preserved and utilised to satisfy the peak cooling demand throughout the day. It is primarily utilised in air conditioning and refrigeration systems. In this instance, the CTES aids in reducing the refrigeration plant's size and cooling capacity, enabling the system to run as efficiently as possible and lowering operating costs.

3.1. Building

There is no doubt that the climate system is warming. Since 1850, none of the previous decades have been warmer than the most recent three, and greenhouse gas (GHG) concentrations have grown. The transition to low-carbon and/or carbon-neutral technology may be accelerated by society lowering the carbon intensity of energy services. Buildings will be crucial since they produce a third of all GHG emissions, along with around 40% of the world's energy needs and 25% of its water [36]. The following discusses in detail the most successful studies published between 2019–2022 that encountered the utilisation of PCMs in CTES of buildings.

A 40% solution of tetra-n-butylammonium bromide (TBAB) was selected by Zou et al. (2019) [37] as a cold energy medium for production because of its appropriate phase transition temperature of 11.81 °C and high latent heat (211.9 J/g). Furthermore, the use of $Na_2HPO_4.12H_2O$ as a nucleating agent reduced the amount of super-cooling experienced by the material; this improved crystallization behaviour could be seen under light microscopy. It has been shown that dimensionally stable TBAB hydrate/fumed silica (SiO_2) CPCMs can be fabricated and described. The results show that the CPCM containing 30% SiO_2 has a high latent heat of 134 J/g, a low undercooling of 2.01 °C, and excellent shape stability, as shown in Figure 1. There is also no liquid leakage above the melting temperature of 8.33 °C, which is a significant advantage.

Philip et al. (2020) [38] created a eutectic PCM for thermal energy storage. They prepared, analysed, and experimented with a new binary eutectic combination. DSC determines the thermo-physical properties of the resulting co-crystals. An 80:20 eutectic mixture of cetyl and lauryl alcohol melts at 20.01 °C with a latent heat of 191.63 J/g. Thermal conductivity was shown to be very good. Figures 2–4 show good results for the thermal stability and reliability testing using the novel combination of accelerated thermal cycling and thermo-gravimetric analysis. The smaller peak near the freezing point of the mixture indicates phase transformation (solid to solid). In the case of cetyl alcohol, one endotherm is observed on heating and two exotherms are observed on cooling the sample. Cetyl alcohol as observed from the DSC curve shows a melting point at 51.5 °C and freezing temperatures of 43.97 and 38.09 °C (Figure 3). Two exotherms are seen on the cooling curve. The first peak depicts liquid-to-rotator phase transition at 43.97 °C and the second peak shows the rotator phase transition to a crystalline structure at 38.09 °C.

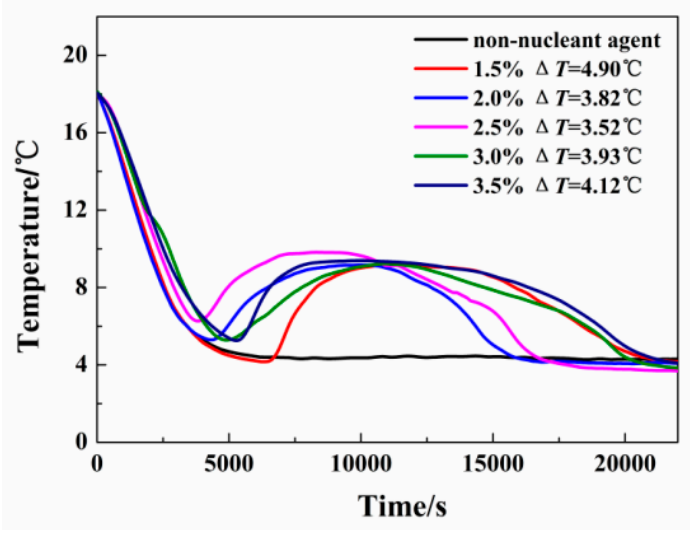

Figure 1. Effect of $Na_2HPO_4 \cdot 12H_2O$ content on the super-cooling degree of TBAB hydrate [37].

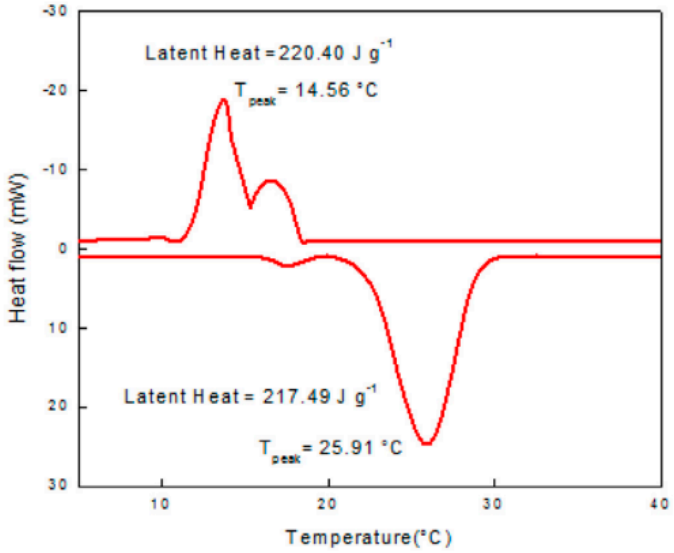

Figure 2. DSC curve of lauryl alcohol [38].

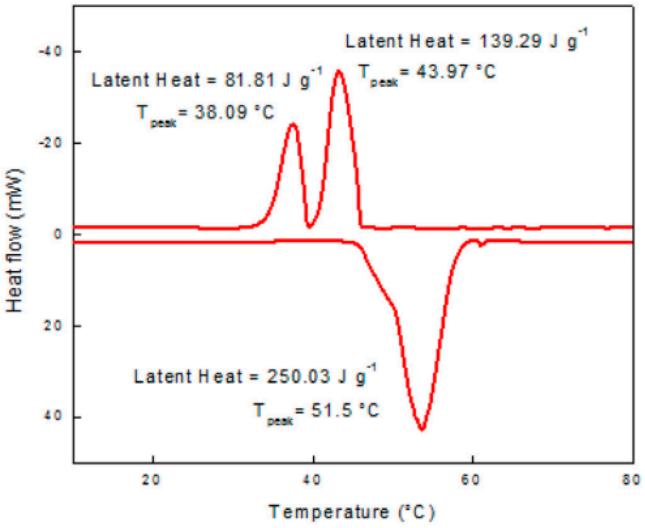

Figure 3. DSC curve of cetyl alcohol [38].

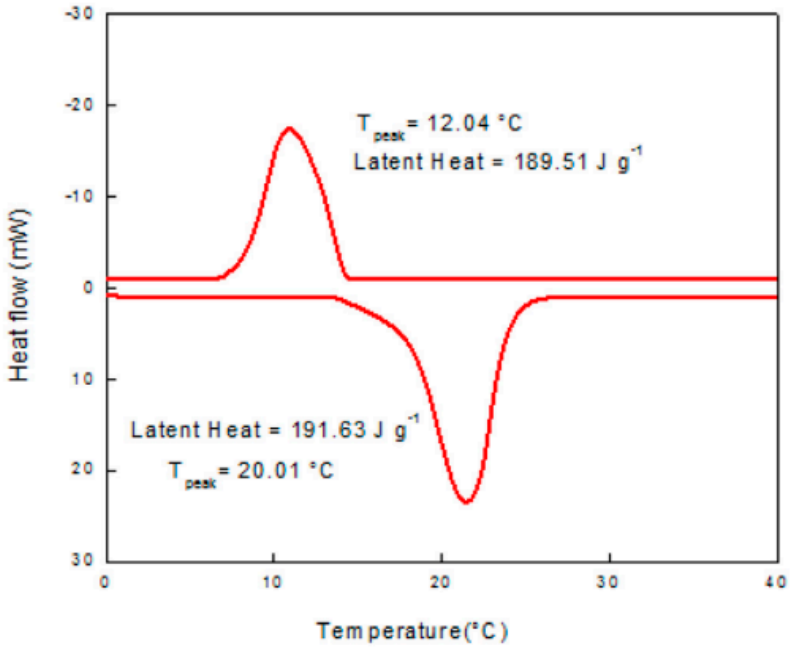

Figure 4. DSC curve of lauryl alcohol–cetyl alcohol eutectic mixture [38].

Jebasingh and Arasu (2020) [39] developed a eutectic PCM suitable for low-temperature applications such as building cooling based on an 85:15 mass ratio of organic fatty acids, capric acid (CA), and myristic acid (MA) and investigated their thermal and chemical stability properties using DSC, Fourier Transform Infrared spectroscopy (FT-IR), thermogravimetric analysis (TGA), and a KD2 Pro thermal property analyser. The fabrication steps are shown in Figure 5. Thermal cycling tests were also performed using the apparatus shown in Figure 6. These properties were compared with fatty acids. DSC testing showed a latent heat capacity of 156.99 J/g and a phase transition temperature of 20.86 °C. The thermal conductivity of the CA–MA PCM is 0.152 W/m K. According to TGA studies, eutectic PCMs are thermally stable. The binary eutectic combination is chemically stable according to FT-IR.

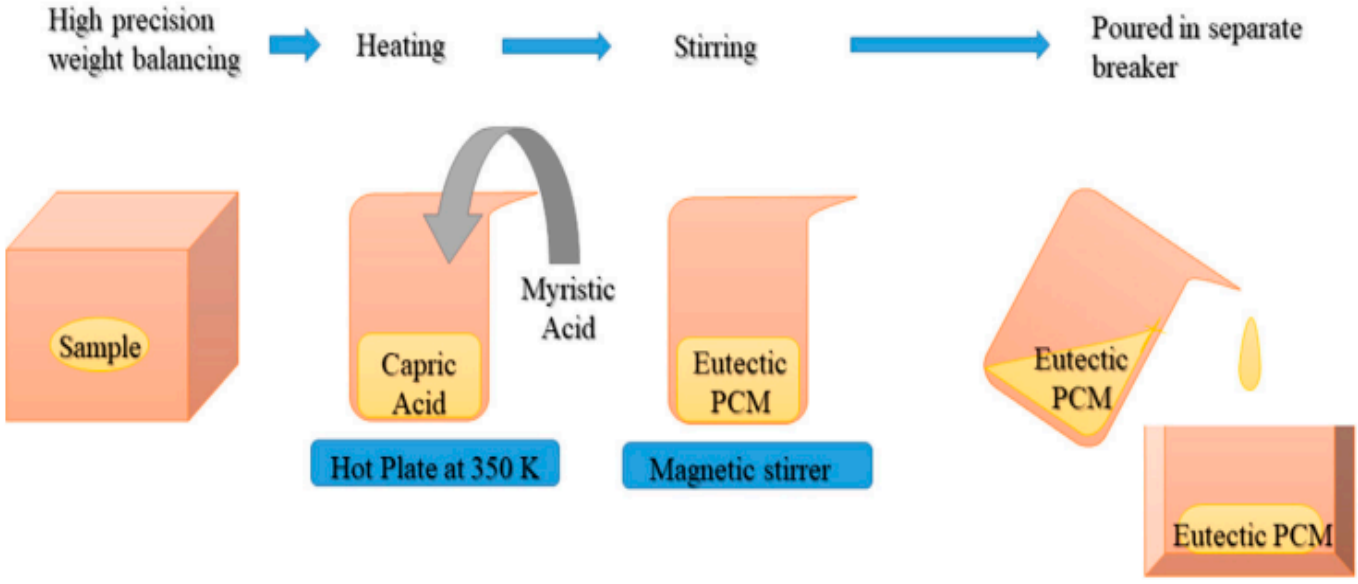

Figure 5. Diagrammatic representation of CA–MA eutectic mixture preparation [39].

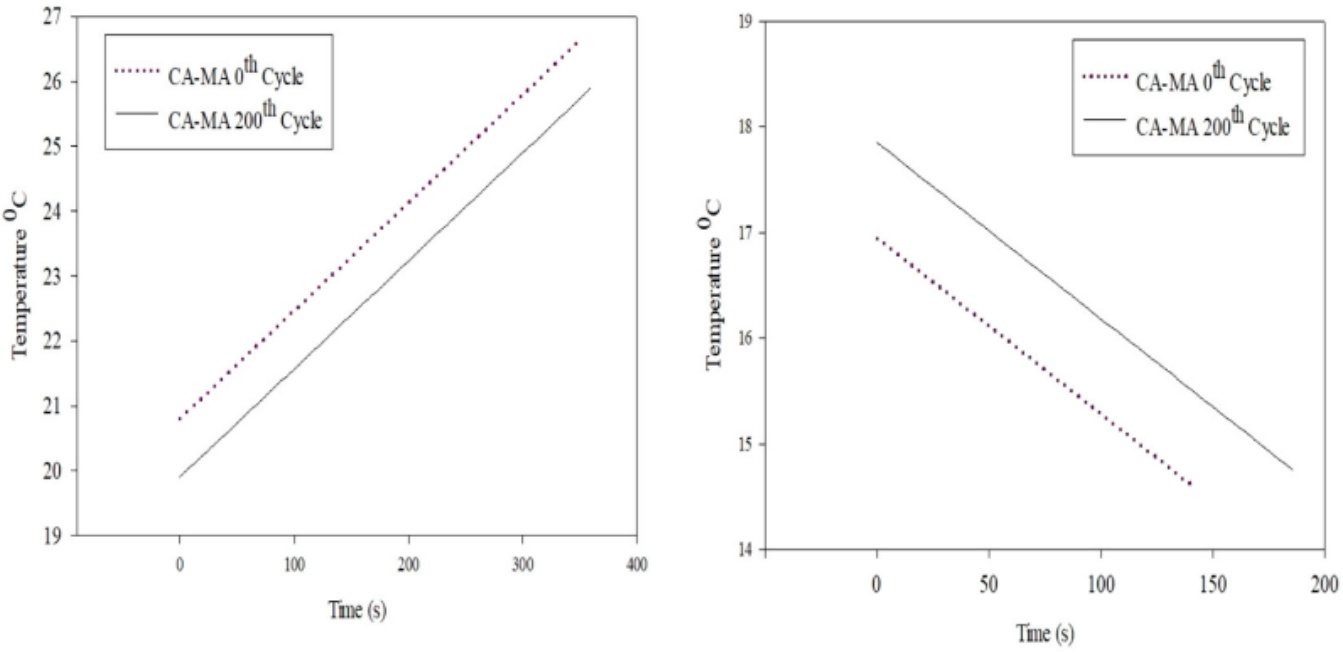

(**a**) (**b**)

Figure 6. The time curve for melting and freezing of CA and CA–MA at the initial conditions: (**a**) Melting and (**b**) Freezing [39].

Alkhwildi et al. (2020) [40] proposed a geothermal heat pump (GHP) system with an integrated hydrate PCM storage tank for cold climate buildings, as shown in Figure 7. PCM storage reduced heat load peaks and annual heat load imbalances in a ground source heat exchanger (GHX), assuming proper installation. In heating mode, the heat pump collects heat from a closed loop to solidify the hydrated PCM. The heat of fusion is stored in PCM tanks and the GHX for daily and seasonal consumption. Electricity meter data from an apartment complex was utilised to forecast space heating, cooling, and hot water demand to test the proposed method. The data were used in a 20-year hourly dynamic life cycle simulation model in TRNSYS software to create an optimal arrangement of GHX and PCM storage designed to balance annual thermal soil loads. The simulation findings indicate that the utilization of PCM tanks has an enormous opportunity to reduce the size of the investigated GHX; nevertheless, owing to the hysteretic heating and cooling profiles, the system is dependent on the PCM melting temperature. Figure 8 shows that of all GHX designs, a PCM melt temperature of 27 °C resulted in the smallest PCM tank capacity.

A new shape-stabilized composite PCM with promising thermal characteristics and an efficient encapsulation method was suggested by Yang et al. (2020) [41]. The use of lauryl alcohol, stearic acid, and nanoparticles denoted as LA–SA/Al_2O_3 to create a binary eutectic PCM with suitable thermal characteristics for buildings was first investigated. Then, the synthesised LA–SA/Al_2O_3 was absorbed into ceramsite and then encapsulated with a styrene–acrylic emulsion and dry cement powder for shape stability. The best ratio of LA–SA/Al_2O_3 is 82 wt.% LA + 18 wt.% SA with 0.5 wt.% Al_2O_3 nanoparticles, with a melting temperature of 21.3 °C and a latent heat of 205.9 kJ/kg. The mechanical performance of the CPCM embedded in concrete with 15 wt.% LA–SA/Al_2O_3/C is satisfactory, and the material showed promise for moderating the effects of the external environment on inside temperatures and decreasing the load on HVAC systems. However, as the PCM's doping level increases, the visible density of the material drops, resulting in a decrease in the maximum stress.

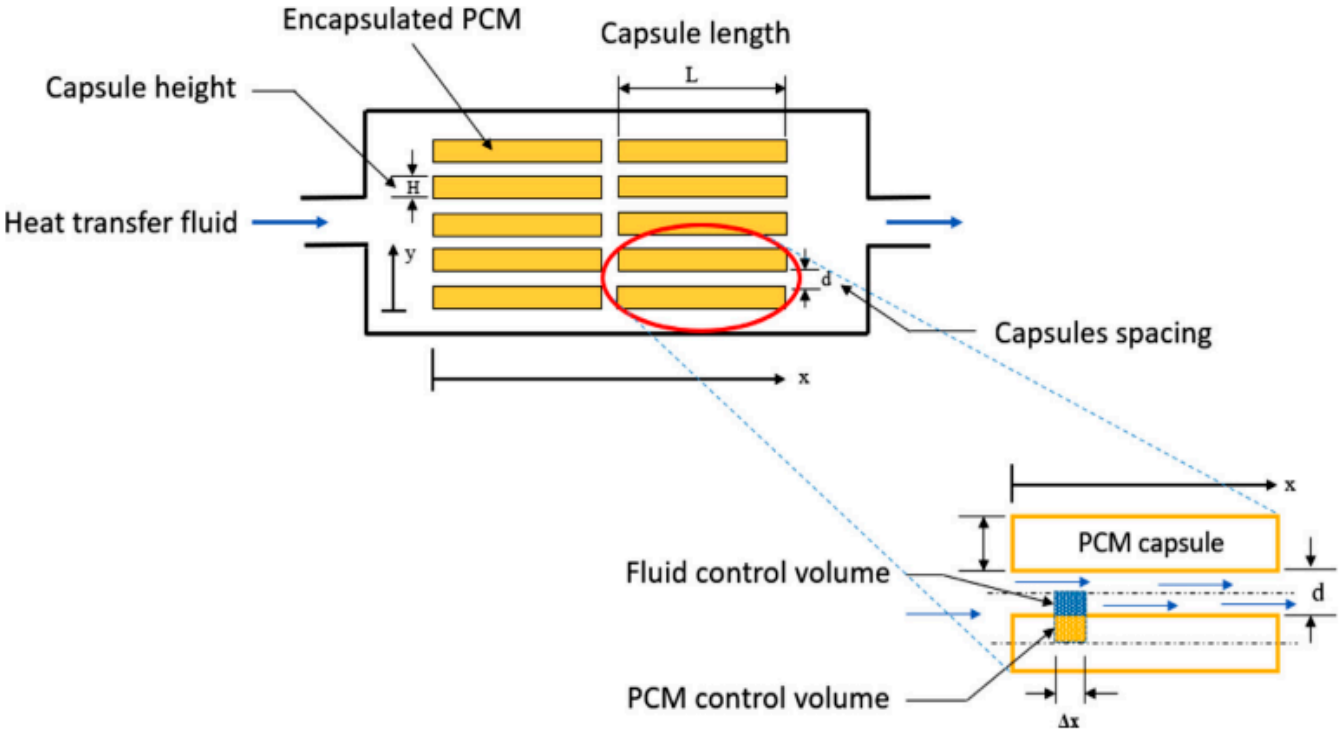

Figure 7. A representation of the storage tank with encapsulated PCM [40].

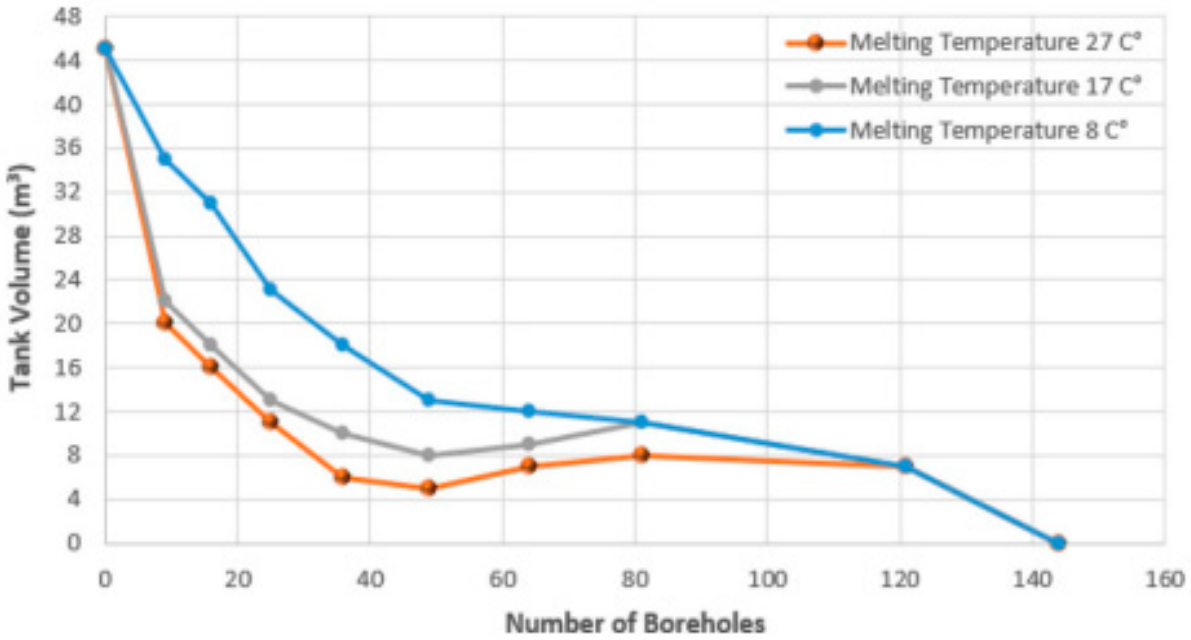

Figure 8. Influence of tank volume on GHX size for different designs of different melting temperatures [40].

Wang et al. (2021) [42] created PCM compositions to reduce phase transition temperature to 20 to 25 °C and improve heat storage and release. After adding $MgCl_2.6H_2O$ as a nucleating agent, $CaCl_2.6H_2O/MgCl_2.6H_2O$ composite phase change materials (CPCMs) were synthesised. $SrCl_2.6H_2O$ was added to reduce the sub-cooling of inorganic PCM. Hydroxyethyl cellulose (HEC) was added to improve material recyclability. Thermogravimetric analysis and differential scanning calorimetry (DSC) were performed on the CPCM to determine the phase transition temperature, thermal properties, degree of sub-

cooling, and thermal cycling properties. The phase transition temperature of the PCM equilibrated by 35% $MgCl_2.6H_2O$, 5% $SrCl_2.6H_2O$, and 0.5% HEC with $CaCl_2.6H_2O$ is 23 °C. The PCM possesses a latent heat of phase change of 130 J/g. Figure 9 shows the standard deviation of latent heat recovery against the number of melting–freezing cycles. This in turn shows that $CaCl_2.6H_2O$ with a sealed hermetic pan has maximum latent heat recovery without a considerable change throughout the cycles. These results are compared significantly against $CaCl_2.6H_2O$ with a small opening in the cove that shows a reduction of around 41% of the latent heat recovery after 100 melting–freezing cycles.

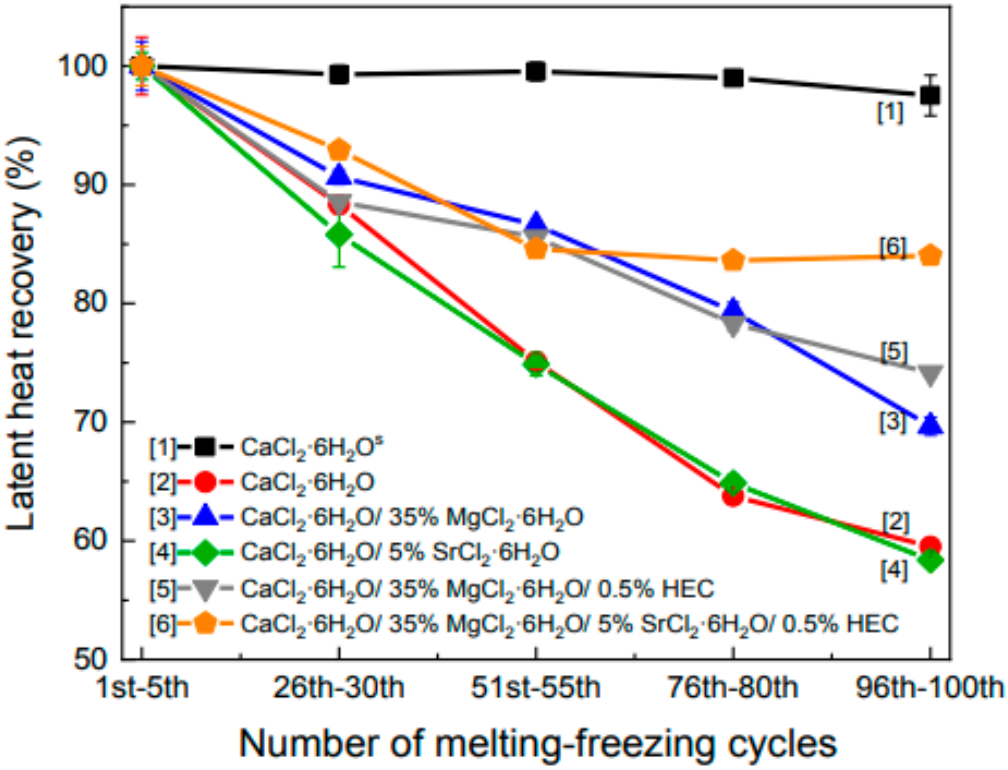

Figure 9. Latent heat recovery of the pure material and CPCMs after typical cycle times [42].

Dong et al. (2022) [43] measured the temperature and phase transition of PCM spheres. The physical model of the PCM sphere was created and validated using CFD simulation tools and experimental data. The validated model simulates the thermal behaviour of a tank filled with PCM spheres. At the same time, the effects of PCM ball diameters (90 and 60 mm) and cold water flow were investigated. Smaller PCM ball diameter and faster chilled water flow rate increase freezing speed. The ideal phase change ball diameters are 90 and 60 mm, and the optimal input flow rate is 2.196 m/h.

According to the study cited in Table 1, a particular PCM's phase transition temperature was reached at 23 °C. Additionally, for all of the GHX configurations, the lowest PCM tank capacity was reached at a temperature of 27 °C. Additionally, by increasing the flow velocity of cold water, a smaller PCM ball diameter enables a greater freezing rate to be attained.

Table 1 summarises previous studies on the utilisation of PCM for cold storage in buildings, including the type of PCM, studied parameters, and findings.

Table 1. A summary of studies on the utilisation of PCMs for cold storage in buildings.

Authors (Year) [Reference]	Configuration/Composition	Study Type	Studied Parameters	Highlighted Results/Findings
Zou et al. (2019) [37]	TBAB hydrate/fumed silica (SiO_2) composite PCM.	Experimental	Effect of $Na_2HPO_4.12H_2O$ content on the super-cooling degree of TBAB hydrate and the nucleating agent on crystalline behaviour of TBAB hydrate.	The form-stable performance of the composite PCM with 30 percent SiO_2 was outstanding, and there was no liquid leakage at temperatures over the melting point (8.33 °C). The latent heat of the composite PCM was 134 J/g, and the super-cooling degree was only 2.01 °C.
Philip et al. (2020) [38]	A eutectic mixture of lauryl alcohol and cetyl alcohol, with the ratio being 80:20.	Experimental	Effect of mixing lauryl alcohol and cetyl alcohol.	The 80:20 eutectic composition of lauryl alcohol and cetyl alcohol with melting temperature of 20.01 °C and latent heat of 191.63 J/g is fit for use in cold thermal energy storage.
Jebasingh et al. (2020) [39]	A mass ratio of 85:15 between capric acid (CA) and myristic acid (MA), both of which belong to the class of organic fatty acids.	Experimental	Effect of the mixing ratio on latent heat capacity, thermal conductivity, and stability.	The phase change temperature was found to be 20.86 °C, and the latent heat capacity was found to be 156.99 J/g.
Alkhwildi et al. (2020) [40]	Low- to moderate-temperature salt hydrate phase change material.	Experimental and Numerical	Tank volume, melt temperature, and GHX size.	The lowest PCM tank capacity was attained with a temperature of 27 °C for all of the GHX setups.
Yang et al. [41]	A binary eutectic PCM of lauryl alcohol, stearic acid, and nanoparticles denoted as LA–SA/Al_2O_3.	Experimental	The influence of mass fraction of LA–SA/Al_2O_3 on the mechanical properties.	The best ratio of LA–SA/Al_2O_3 is 82 wt.% LA + 18 wt.% SA with 0.5 wt% Al_2O_3 nanoparticles, with a melting temperature of 21.3 °C and a latent heat of 205.9 kJ/kg.
Wang et al. (2021) [42]	$SrCl_2.6H_2O$ was added to PCMs (CPCMs) of the $CaCl_2.6H_2O/MgCl_2.6H_2O$ binary salt system in order to lower the super-cooling degree of inorganic PCM.	Experimental	Effect of adding $MgCl_2$ $6H_2O$ and $SrCl_2$ $6H_2O$.	At a temperature of 23 °C, the phase transition temperature of the PCM was achieved by combining 35% $MgCl_2.6H_2O$, 5% $SrCl_2.6H_2O$, and 0.50% HEC in a solution that was balanced by $CaCl_2.6H_2O$.
Dong et al. (2022) [43]	Cold energy storage tank filled with multiple PCM balls.	Experimental and Numerical	Ball diameter of PCM and flow rate of chilled water.	A lower PCM ball diameter allows for a higher freezing rate to be obtained, which may be accomplished by increasing the flow velocity of cold water.

3.2. Air Conditioning and Refrigeration

Luxurious and contemporary living standards are made possible by high energy use. More than half of the power used by building service systems goes toward air conditioning systems. Traditional air conditioning systems rely on non-renewable energy sources for operation. In contrast, the use of clean energy may solve the issues of energy consumption and environmental degradation. The use of a solar-powered air conditioning system has, therefore, been selected as a preferred refrigeration technology. Because solar energy is sporadic and has a low energy density, it is effective to utilise the extra solar energy produced throughout the day and store it for use at night, or to store solar energy during the summer and use it in the winter, when energy production and consumption are not

coordinated. It is suggested to use a solar energy storage system. Some research carried out theoretical analysis and experiments to address relevant issues [44]. The next sections elaborate on the most successful studies published between 2018–2022 that discussed the utilisation of PCMs in CTES for air conditioning and refrigeration.

Jiang et al. (2018) [45] investigated the heat transport and cold storage performance of a falling film type. The experimental setup combines falling film heat transfer and cold storage with solid–liquid PCMs. Each horizontal column has 36 copper pipes. The copper pipes are coated with a hydrophilic coating to minimize the solid–liquid contact angle. The heat transfer fluid is water, a mixture of capric acid, lauric acid, and oleic acid with a liquid film. The Reynolds number range of liquid film was from 100–500 and the phase transition temperature was around 20 °C. Cold energy regenerators provide high heat transfer and cold storage with low pump capacity. Figure 10 shows that lowering the Reynolds number of the film improves refrigeration performance.

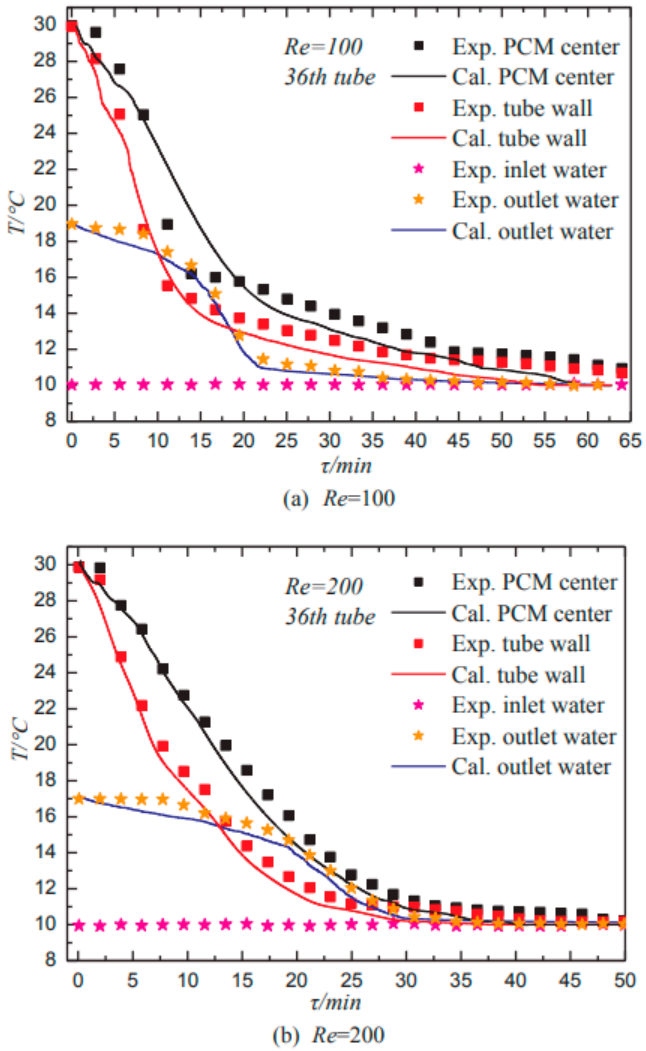

Figure 10. Temperature assessment of calculated and experimental values for 36th tube in cold energy storage process [45].

Said and Hassan (2018) [46] developed a new method to integrate thermal energy storage made using PCMs into conservative AC systems to improve cooling capacity. This technology integrates a phase change board with an AC capacitor. The charging and discharging process is affected by the plate configuration of the PCM, the air intake velocity, and the temperature. It is also shown how these settings affect the performance of air conditioners. Figure 11 presents the variation of the coefficient of performance

(COP) of the AC system against operational time for various PCM plate configurations while using different inlet air temperatures of 35 °C, 40 °C, and 45 °C. Also, Figure 12 shows the COP of a conventional AC system without using a PCM heat exchanger for the considered parameters. Specifically, the COP decreases with time and inlet air temperature. Furthermore, all configurations of the AC unit with PCM have COP values that are higher than those of the conventional AC unit at any given instant. Furthermore, at various configurations, the performance coefficient of an air conditioning unit using PCMs at an inlet air temperature of 35 °C outperforms the conventional one by 14%, 13%, and 12% at inlet velocities of 0.96 m/s, 1.2 m/s, and 1.44 m/s, respectively.

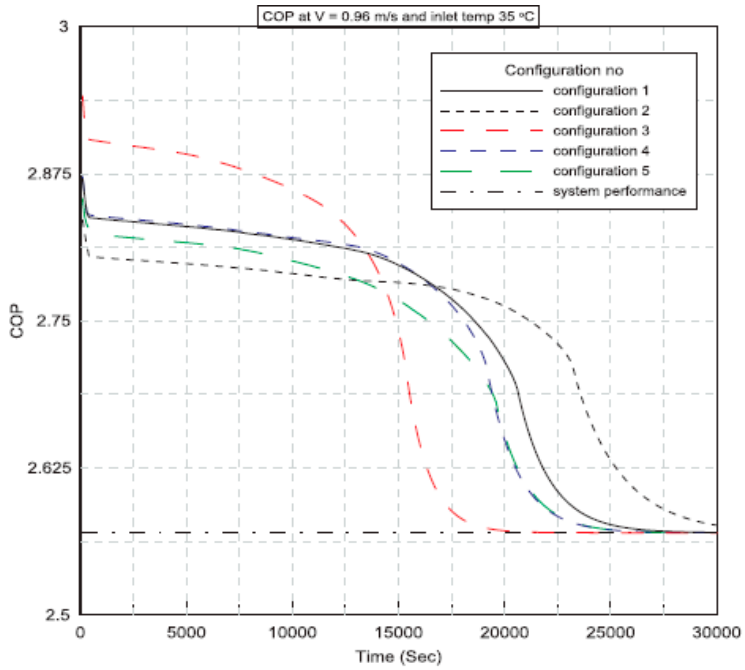

(a) 35 °C

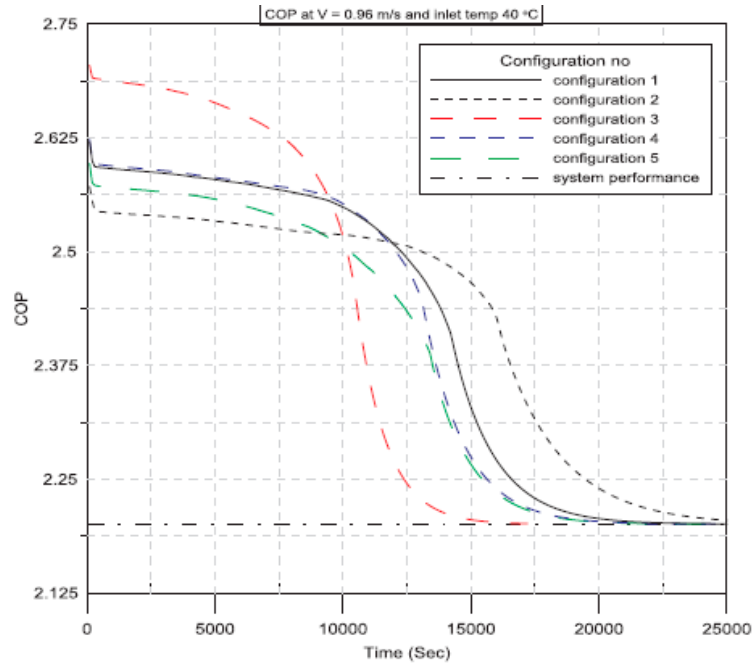

(b) 40 °C

Figure 11. *Cont.*

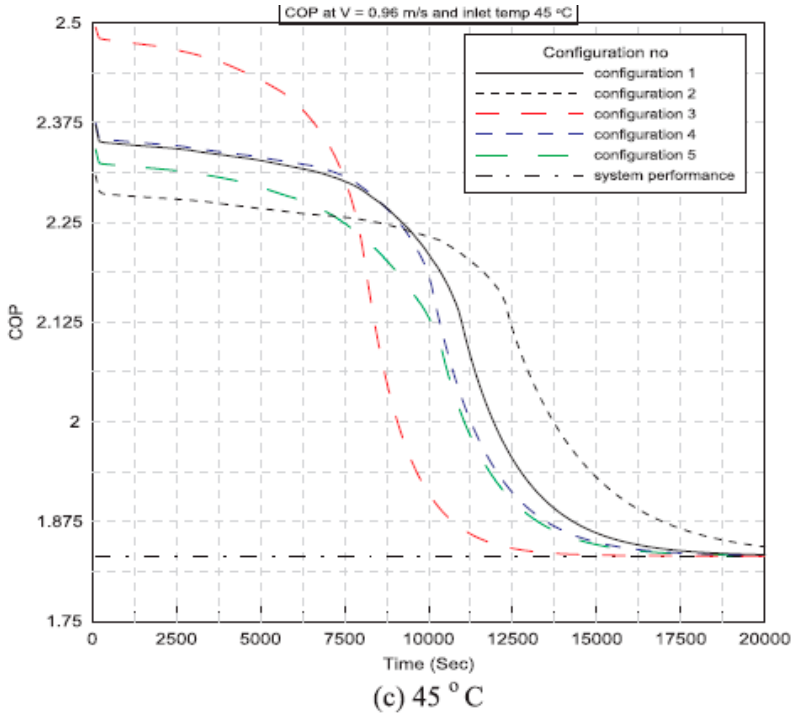

Figure 11. Variation of coefficient of performance against time at V = 0.96 m/s and different inlet air temperatures: (**a**) 35 °C, (**b**) 40 °C, and (**c**) 45 °C [46].

Sunxi et al. (2019) [47] used an octanoic acid–myristic acid binary eutectic mixture (OA–MA) as the base liquid. A PCM with a unique shape of OA–MA/expanded graphite (EG) (OA–MA:EG = 93:7) was formed by uniform absorption of OA–MA into the porous structure of EG. Scanning electronic microscopy (SEM) shows the microstructure. DSC measured the phase change temperature (PCT) and latent heat. The Hot Disk thermal constant analyser analysed the thermal conductivity. OA–MA/EG stability was verified by 100 thermal cycling tests. The transition temperature of the OA–MA phase is 7.1 °C and its thermal conductivity is 0.2971 W/m K. The transition temperature of the OA–MA/EG phase EG is 6.8 °C, the latent heat is 136.3 J/g, and the thermal conductivity is 0.9975 W/m K, which is 2.36 times that of OA–MA. Thermal cycling studies demonstrate the thermal durability of the OA–MA/EG PCM.

Xie et al. (2020) [48] prepared a unique type of composite PCM using MEG to adsorb a $K_2HPO_4.3H_2O$–$NaH_2PO_4.2H_2O$–$Na_2S_2O_3.5H_2O$–H_2O eutectic salt using an impregnation technique. As shown in Figure 12, the eutectic salt adsorption capacity of MEG at 120 min was 75.33% higher than that of unmodified expanded graphite (EG). The phase transition temperature of the composite phase change material (PCM) is −5.30 °C, the significant latent heat is 161.8 kJ/kg, and the super-cooling degree is 1.83 °C. The thermal conductivity of the composite PCM is 13.3 times higher than that of the eutectic salt. In addition, thermal cycling tests show that thermal reliability is quite high, as shown in Figure 13.

Karthikeyan et al. (2021) [49] prepared a combination of capric, lauric, and oleic acids to produce low-temperature PCMs for refrigeration applications. As shown in Figure 14, an experimental study was conducted in a double-helix thermal storage unit (CTESU) to analyse the charge and discharge behaviour of the combination of capric, lauric, and oleic acid. It was found that the melting time of the PCM is meaningfully longer at heat transfer fluid (HTF) inlet temperatures of 30 °C and 35 °C than at a HTF inlet temperature of 40 °C. Similarly, the melt rate increases with increasing HTF flow rate. As shown in Figure 15, when the HTF inlet flow rate was increased from 2 L/min to 3 L/min at a temperature of 30 °C, the melt rate decreased by 3.5%, while the HTF inlet flow rate decreased by 10%. The melting rate exists at a temperature of 40 °C.

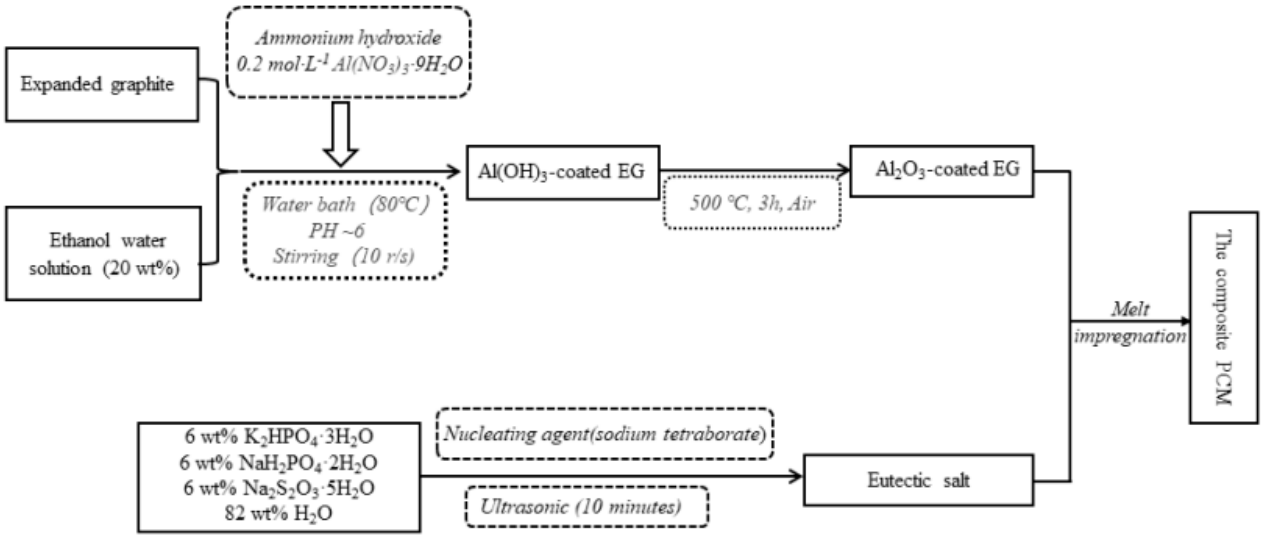

Figure 12. Schematic diagram of the preparation of the composite PCM [48].

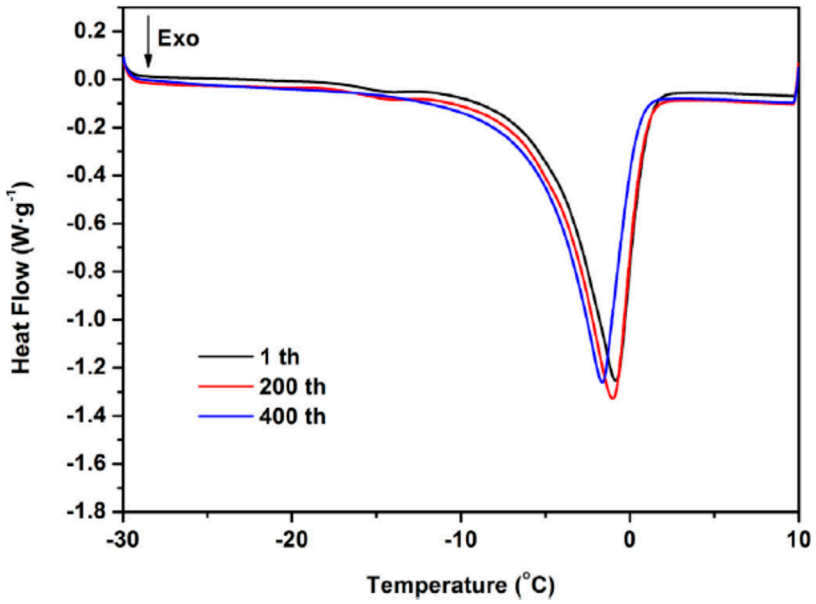

Figure 13. DSC curves of the composite PCM at 1st, 200th, and 400th thermal cycles [48].

To reduce energy consumption, Ghodrati et al. (2022) [50] used both water and ethylene glycol which were considered as potential PCMs for cold energy charge storage. According to this, when using water as the PCM, the system used only 63% of the available energy during the first 100 min, but without the PCM, the system used about 90.9% of the available energy after the first 100 min. If the water is replaced with ethylene, the system loses only 35.97% of the total energy in the first 500 min; the remaining charge is retained.

Selvnes et al. (2022) [51] report on the scheme and performance of CTES. Their process consists of a pillow plate heat exchanger (PP-HEX) immersed in storage medium of a low-temperature PCM. The charge–discharge performance of a CTES device with plates in a tank was thoroughly tested using carbon dioxide (CO_2) as the refrigerant and a commercially available PCM with a phase change temperature of −9.6 °C. From Figure 16, it can be seen that, at the same refrigerant evaporation temperature, comparing 15 mm and 30 mm plate spacing designs, the 15 mm charge time is faster than the 30 mm charge time. This is due to the fact that employing the 30 mm design doubles the theoretical potential storage capacity of the CTES unit. Compared to the 15 mm design, the 30 mm configuration

takes about 150% longer to charge than the 15 mm configuration at −13 °C. The measured charge time increase at 30 mm is approximately 161% higher than expected for a T_{CO2} evaporation temperature of −20 °C.

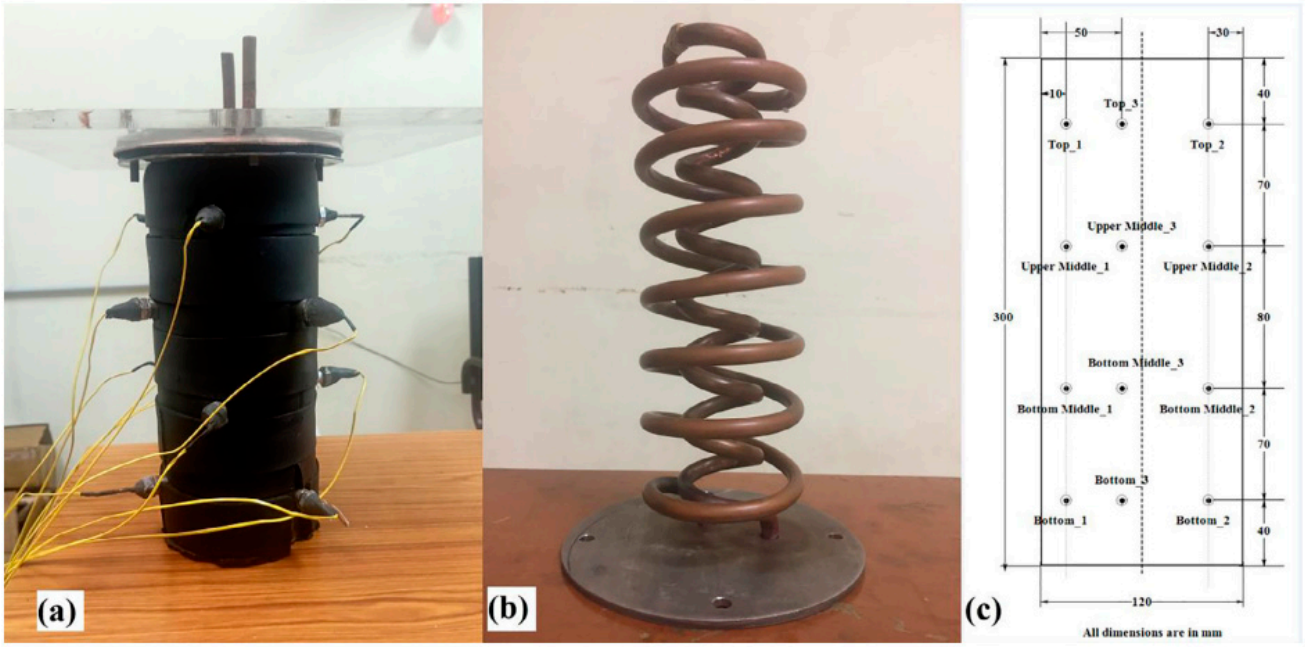

Figure 14. Pictorial view of (**a**) CTESU, (**b**) double-helix coil, and (**c**) layout of the location of thermocouples in CTESU [49].

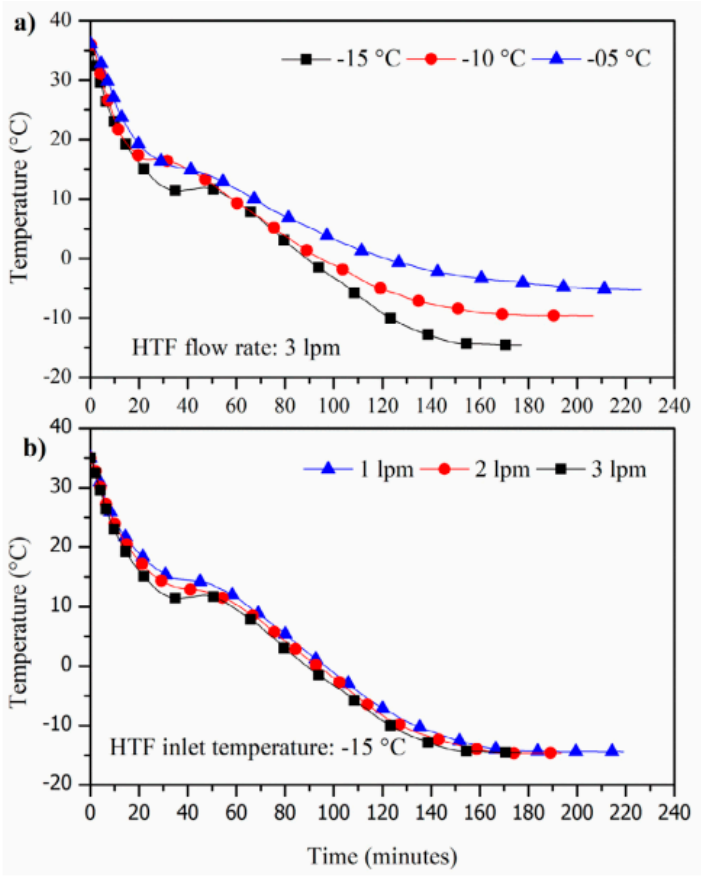

Figure 15. Influence of (**a**) HTF inlet temperature and (**b**) flowrate during the charging process [49].

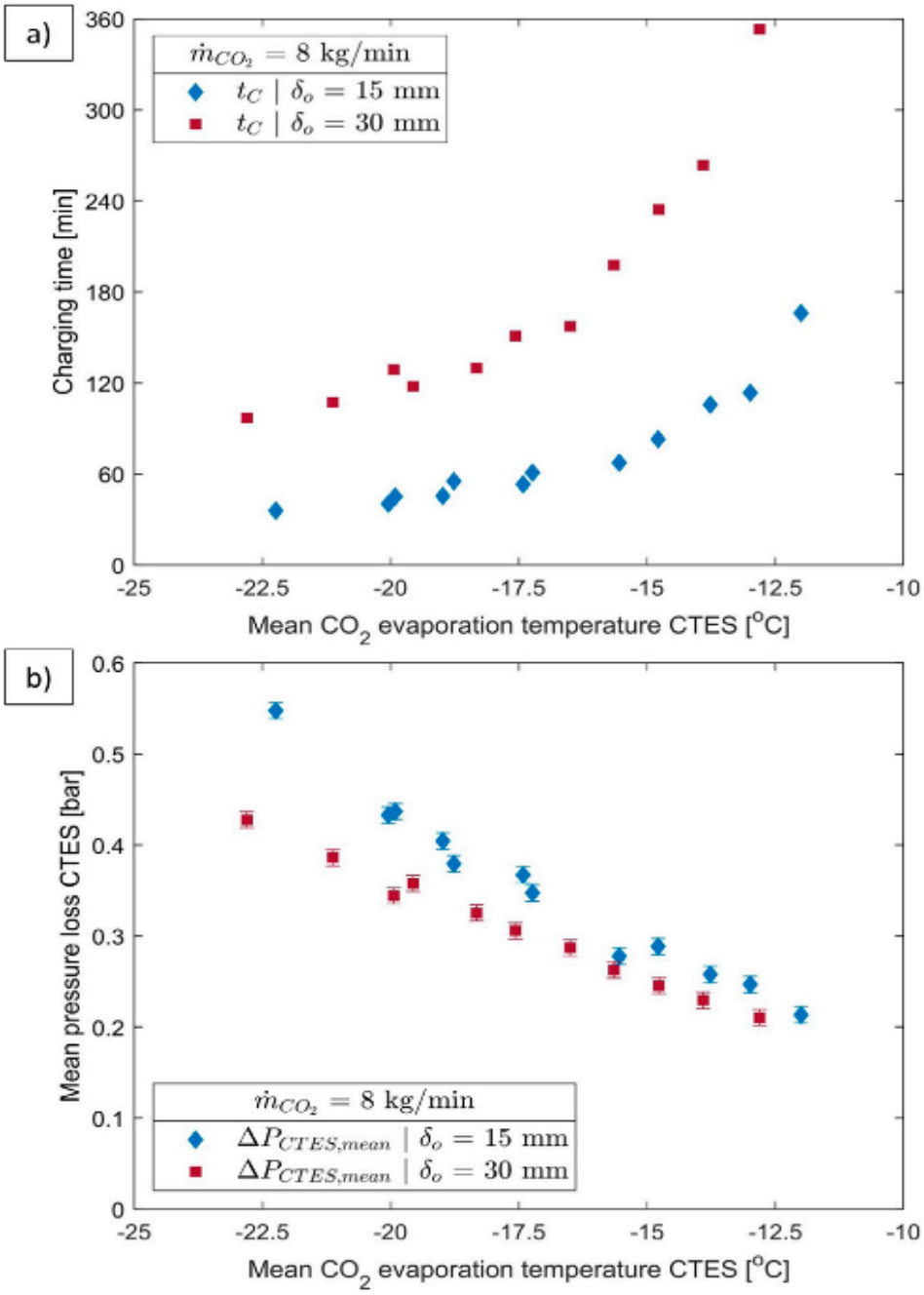

Figure 16. The influence of refrigerant evaporation temperature for the 15 mm and 30 mm configurations with 8 kg/min refrigerant mass flow rate on (**a**) the charging time and (**b**) mean pressure loss [51].

Zheng et al. (2022) [52] constructed an air-cooling system for phase change microcapsule cold storage. The encapsulated phase change material was combined with thermally conductive water to form a microcapsule suspension. Three highly stable microcapsule PCM suspensions were prepared. Analysis determined the thermo-physical properties of the suspensions. The cold storage performance of the phase change microcapsule suspensions was tested in the cold storage of the composite systems. The optimal composition ratios of the base fluid were 99.1% deionized water, 0.2% SDS, 0.2% xanthan gum, and 0.5% NaCl. The capacity of the phase change cold storage is 1.5 times that of the ice cold storage, and it is more powerful overall.

Table 2 summarises previous studies on the utilization of PCM for cold storage in air conditioning and refrigeration, including the type of PCMs, studied parameters, and findings.

Table 2. A summary of studies on the utilisation of PCMs for cold storage in air conditioning and refrigeration.

Authors (Year) [Reference]	Configuration/Composition	Study Type	Studied Parameters	Highlighted Results/Findings
Jiang et al. (2018) [45]	Mixture of decanoic acid, lauric acid, and oleic acid.	Experimental and Numerical	Pumping power and film Reynolds number.	The cold energy regenerator has excellent heat transfer performance as well as cold storage properties while using a minimal amount of pumping power.
Said et al. (2018) [46]	Integrating plates of PCM with a condenser of an air conditioning unit.	Experimental	Configurations of PCM plates, as well as the velocity and temperature of the air that enters the PCM plates, are all taken into consideration.	At various configurations, the PCM-equipped air conditioner outperforms the conventional unit by 14%, 13%, and 12%at inlet velocities of 0.96 m/s, 1.2 m/s, and 1.44 m/s, respectively for an inlet air temperature of 35 °C.
Sunxi et al. (2019) [47]	PCM of OA–MA and EG with the ideal mass ratio of 93:7 (OA–MA:EG).	Experimental	Effect of adding EG into OA–MA.	The OA–MA/EG composite PCM demonstrated a high degree of thermal resilience when subjected to thermal cycle testing.
Xie et al. (2020) [48]	$K_2HPO_4 \cdot 3H_2O$–$NaH_2PO4 \cdot 2H_2O$–$Na_2S_2O_3 \cdot 5H_2O$–H_2O eutectic salt/MEG composite PCM.	Experimental	Mass fraction and thermal cycles.	Tests with a thermal cycle duration of 400 times indicated that the composite PCM had outstanding thermal reliability.
Karthikeyan et al. (2021) [49]	Capric–lauric acid/oleic acid combination.	Experimental	The inlet temperature and flow rate of HTF.	When the flow rate of HTF during the discharging process was increased, the melting rate increased by 16 percentage points in comparison to lower flow rates. On the other hand, despite the overall rise in flow rates, the charge rate did not shift considerably. When compared to the HTF intake temperature of −15 °C, the solidification of PCM at temperatures of −5 and −10 °C requires much more time.
Ghodrati et al. (2022) [50]	Two PCMs of water and ethylene glycol.	Experimental	Effect of using water and ethylene glycol as PCMs.	When water is used as the PCM for the first 100 min, the system only uses 63% of its total energy; however, when there is no PCM present, the system loses roughly 90.9% of its total energy after the first 100 min. When water is replaced with ethylene, the first 500 min of the reaction only results in the release of 35.97% of the system's total potential energy.
Selvnes et al. (2022) [51]	Commercial PCM with phase change temperature of −9.6 ∘C.	Experimental	Effect of pitch of pillow plate heat exchanger on charging and discharging of PCM, refrigerant evaporation temperature.	The use of a plate pitch of 30 mm produced the greatest mean discharge rate and the highest total discharged energy throughout the course of the cycle with 9.79 kilowatts and 17.04 kilowatt hours, respectively. Charging time for the 30 mm design was risen by about 150% compared to when it was used at an evaporation temperature of −13 °C.
Zheng et al. (2022) [52]	To create phase change microcapsule suspensions with mass fractions of 5%, 10%, and 15%, PCMs were encapsulated and then combined with water and had strong thermal conductivity.	Experimental	Effect of adding wt.% of SDS, xanthan gum, and NaCl to deionized water.	99.1% deionized water, 0.2% SDS, 0.2% xanthan gum, and 0.5% NaCl made the optimum base liquid. System cooling capacity dropped. Phase change cold storage offers 1.5 times the capacity of ice cold storage and performs better overall.

This review, in regard to various works of research and summarised in Table 2, shows that cold energy regenerators have high heat transfer performance and cold storage capabil-

ities while requiring a low amount of pumping power. Additionally, a further experiment's usage of 30 mm plate pitches produced the greatest mean discharge rates and total energy released. Additionally, the melting rate rose by 16 percentage points in contrast to lower flow rates when the rate at which HTF was discharged was increased.

3.3. Food Storage

For the greatest preservation of food's natural colour, appearance, taste, nutritional content, and other attributes, quick freezing has long been acknowledged as the optimum technique of food preservation. Food may be frozen more quickly and with fewer ice crystals thanks to this procedure. As a result, less time is needed to reach the threshold where the creation of ice crystals is at its peak, and water is prevented from recrystallizing and cell membranes from being damaged (squeezing or rupturing). Commercially frozen foods are often "rapid frozen" utilizing a variety of tools, including fluidized freezing beds, air blast freezers (ABFs), and plate freezers [53]. The coming sections present a rich analysis of the most successful studies published in 2021 that discuss the utilisation of PCMs in CTES for food storage.

Tas and Unal (2021) [54] developed a nano-hybrid of PCMs and halloysite nanotubes (HNT) to produce nano-fillers with thermal buffering capabilities. As shown in Figure 17, HNTs were soaked with polymeric PCMs such as PEG400 and PEG600. This process results in the formation of a mixture of HNT/PCM nano-hybrids with durable shapes. Melt compounding was used to encapsulate the combination of HNT/PEG400 and HNT/PEG600 nano-compounds in a polyethylene (PE) matrix. This resulted in flexible nanocomposite films. Frozen nanocomposite sheets thawed at room temperature at a much slower rate than bare PE sheets. The gap is less than half. In addition, the nanocomposite film was 18 and 20 min more effective in delaying the freezing and heating of cold samples, respectively, compared to the normal PE film. Individually, the HNT/PEG400 and HNT/PEG600 nano-hybrids show melting transitions in the temperature range of −22.0–6.4 °C and −6.0–19.0 °C, respectively. On the other hand, the melt transition of the HNT/polyethylene glycol (PEG)-M nano-hybrid has a wide temperature range from −21.8 °C to 21.7 °C, as shown in Figure 18.

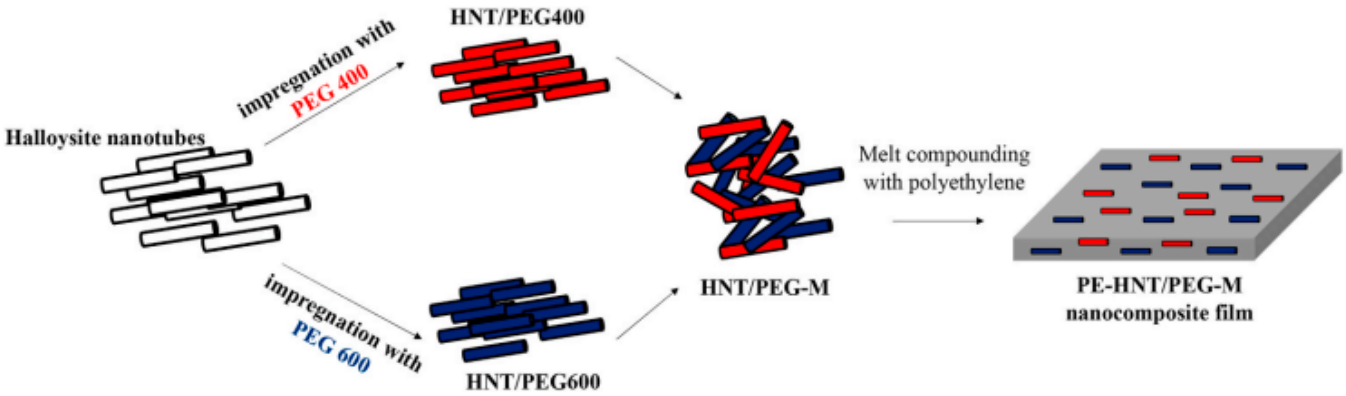

Figure 17. Scheme of nanocomposite films [54].

Zhan et al. (2021) [55] investigated the preparation, characterization, and modification of PCMs. Organic PCMs were formed by adding D-(+)-glucos, glycine, and D-sorbitol to 1% NaCl. A simple experimental method was developed to prepare organic PCMs for cold chain logistics. A solution of 5% glycine and 1% NaCl constitutes a good PCM. This PCM has a phase transition temperature of −5.94 °C and a thermal conductivity of 0.58 W(mK). After 50 cycles, the phase transition temperature of the solution was −6.72 °C. After 50 cycles, the activation energy (ΔH) in 5% glycine–1% NaCl was 275.79 J/g, i.e., 15.63 J/g less than before cycling. The ΔH and phase transition temperature of 5% glycine–1% NaCl did not change considerably before and after cycling.

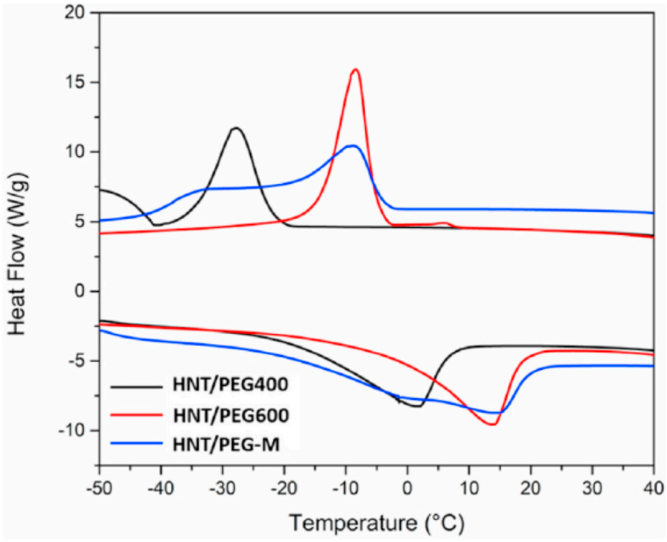

Figure 18. DSC curves of HNT/PCM Nano-hybrids [54].

Table 3 summarises previous studies on the utilisation of PCM in food, including the type of PCMs, studied parameters, and findings.

Table 3. A summary of studies on the utilisation of PCMs for cold storage of food.

Authors (Year) [Reference]	Configuration/Composition	Study Type	Studied Parameters	Highlighted Results/Findings
Tas and Unal (2021) [54]	HNTs that have been impregnated with polymeric PCMs, as well as PEG400 and PEG600.	Experimental	PCM impregnation ratios.	Individual HNT/PEG400 and HNT/PEG600 nano-hybrids showed melting transitions between 22.0 °C and 6.4 °C and 6.0 °C and 19.0 °C, respectively.
Zhan et al. (2021) [55]	Adding edible additives (D-(+)-glucos, glycine, and D-sorbitol) to a 1% NaCl solution.	Experimental	The wt.% of glycine–1% NaCl solution.	After going through 50 cycles, the solution containing 5% glycine and 1% NaCl had a phase transition temperature of −6.72 °C and an activation energy (ΔH) of 275.79 J/g. Before and after cycling, there is not a discernible change in either the glycine concentration or the temperature at which the phase transition occurs in the solution that contains 5% glycine and 1% NaCl.

Regarding the various works of research, including those in Table 3, a solution with 5% glycine and 1% NaCl exhibited a phase transition temperature of −6.72 °C and an activation energy (ΔH) of 275.79 J/g after 50 cycles. In addition, neither the temperature at which the phase transition takes place in the solution containing 5% glycine and 1% NaCl nor the glycine content are noticeably different before and after cycling.

3.4. Cold Chain Applications

Fresh fruit and vegetable consumption has dramatically increased in recent years. It is commonly known that a cold chain may extend the period of time that fresh goods and medications can be stored while maintaining their functionality and freshness and lowering the danger of quality deterioration. According to reports, a third of the fresh food produced worldwide is lost owing to inappropriate temperature storage and transportation. The effective utilization of a cold chain, especially during transit, might help solve the problem by ensuring the safety and quality of the food [56]. The following sections detail the most effective experimental and numerical studies published between 2019–2022 that used PCMs in CTES for cold chain applications.

Song et al. (2019) [57] developed a shape-stabilized PCM with dodecane as a PCM and expanded graphite (EG) as a skeleton. Heat treatment and DSC testing indicated that

16 wt.% was the ideal EG concentration for the composite. Figure 19 shows the shape-stable PCM made of dodecane and expanded graphite (EG). Figure 20 shows that the shape-stable dodecane/EG PCM has a phase transition temperature of −9.67 °C and a latent heat of 151.7 J/g. SEM, FT-IR, and specific surface area analyser data showed that the dodecane was uniformly packed in the EG pores under physical exposure. The thermal conductivity of dodecane/EG is 15 times that of dodecane. Thermal performance testing confirmed the improved thermal conductivity of the PCM composite. A numerical model of the dodecane/EG PCM passive energy storage system was built, and the simulation results were consistent with experimental results.

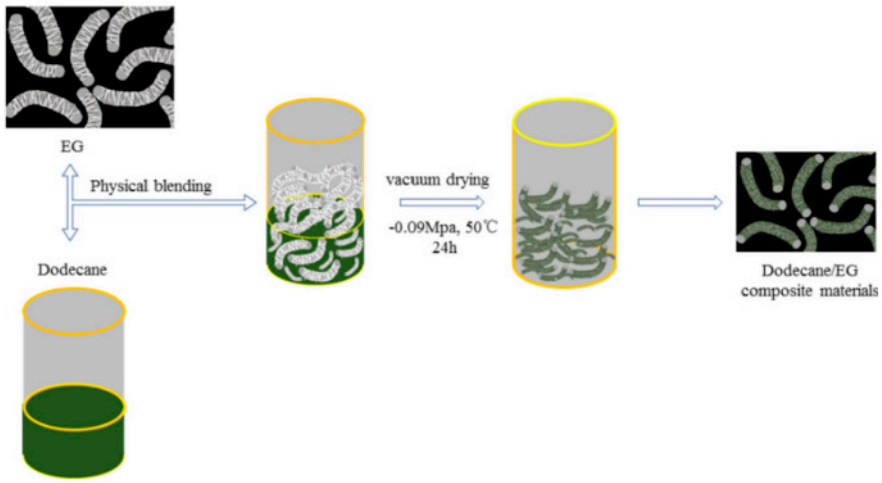

Figure 19. Preparation route of dodecane/EG PCMs [57].

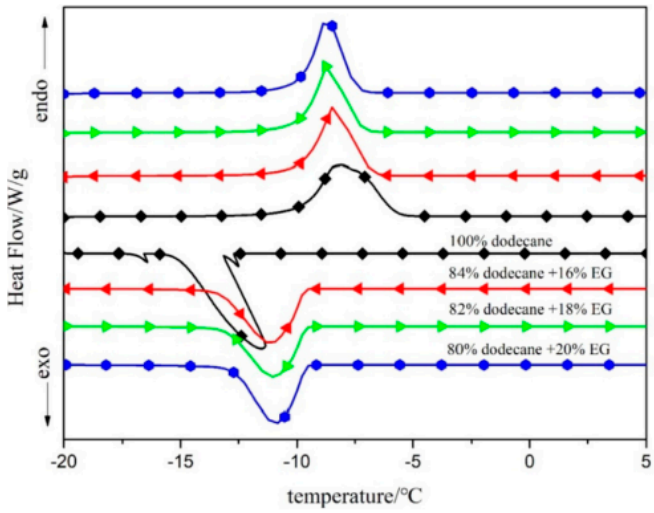

Figure 20. DSC curves of dodecane/EG PCMs [57].

Xiaofeng and Xuelai (2020) [58] developed a multi-temperature PCM cooler. The phase transition temperatures of PCM1 (*n*-octanoic acid–myristic acid complex) and PCM2 (potassium sorbate–water complex) are 7.1 and −2.5 °C, the latent heat values are 146.1 and 256.2 J/g, and the thermal conductivities are 0.2832 and 0.9427 W/m K, respectively. The manufacture of multi-zone coolers was combined using vacuum insulation. The melting process of PCMs was investigated by means of a three-dimensional unsteady model. Good supply practice (GSP) has led to the Insulated Box Temperature Test system. Incubator temperature zones 2 (middle zone) and 3 (low zone) can remain cold for 13 h and 14 h, respectively.

To achieve efficient cold storage for cold chain transportation, Liu et al. (2022) [59] proposed a unique saline phase change material gel (BPCMG) by loading eutectic saline into a

superabsorbent polymer (SAP). Potassium chloride (KCl) and ammonium chloride (NH_4Cl) dissolve in water to form a eutectic PCM brine. This is because the phase transition temperature of the PCM is close to 21 °C, making it ideal for transporting biological samples and aquatic products that require refrigeration. The resulting BPCMGs show that super-cooling has been eliminated, they have a high latent heat of 230.62 J/g, they have a high thermal conductivity of 0.589 W/m K, and they have a high cost-effectiveness of 7.63×10^{-6} $/J. When the total cold storage capacity was 691,800 joules, the longest refrigeration time for aquatic products and biological samples was 21.44 h and 16.37 h, respectively.

Ma et al. (2022) [60] used an organic–inorganic composite PCM containing an aqueous solution of mannitol for energy storage. A saline–alkali solution with a phase transition temperature of 6 °C and a latent heat of 240.1 J/g was produced after adding $MgCl_2$ as a coolant. Nano-CuO and MWCNT-OH were introduced as thermal conductivity enhancers in nanocomposite phase change materials (NCPCM) to improve thermal conductivity and refrigeration efficiency. SDBS (sodium dodecyl benzene sulfonate), PAM (polyacrylamide), and GG (guar gum) are used as dispersants in the base solution for effective dispersion. The dispersing activity of SDBS in brine is poor, but the polymer dispersants are better than PAM and GG. The thermal characteristics and cycling stability of NPCM were also investigated. Mannitol/$MgCl_2$@MWCNT-OH/PAM exhibited the highest thermal performance with a thermal conductivity of 0.685 W/m K and a 57.3% reduction in refrigeration time.

Lin et al. (2022) [61] prepared sodium sulphate decahydrate (SSD, Na_2SO_4–$10H_2O$) for cold chain transportation (2–8 °C). KCl and NH_4Cl lowered their phase transition temperatures, while CMC (carboxymethyl cellulose) and borax (B) hindered phase separation and super-cooling. The microstructure and chemical structure of the composite material presented chemical compatibility. The preferred composite (SSD-BCKN3) shows minimal phase separation, a sub-cooling degree of 0.7 °C, and a phase transition temperature of 6.8 °C.

Chang et al. (2022) [62] used a two-step in situ polymerization method to synthesise microcapsules of poly (urea-formaldehyde) (UF). Here, *n*-tetradecane was applied as a base material, and SDS was used as an emulsifier. The findings show that when the mass fraction of SDS is 1.2%, the initial pH is 3.5, and the mass ratio of core to the shell is 2:1, the phase change microcapsules have strong dispersibility. After the mass fraction of ethanol in the base liquid reaches about 74% by weight, a stable latent heat functional fluid can be produced. An increase in temperature leads to an increase in the thermal conductivity of the latent heat functional fluid, while an increase in the mass fraction of microcapsules leads to a decrease in thermal conductivity. Its viscosity increases with increasing temperature or by increasing the mass fraction of microcapsules.

Ikutegbe et al. (2022) [63] encapsulated low-melting-point PCMs using a UV-PFA (ultraviolet perfluoroalkoxy) coil reactor. Pure Temp (PT) 6 and cross-linked polymethyl methacrylate are used as PCMs or housing materials. Various synthesis factors such as polymerization time and core–shell mass ratio were investigated. The peak melting temperature of 87.4% microencapsulated PCMs (m-PCMs) was 8.2 °C and the average latent heat was 131.1 kJ/kg. Microcapsules deteriorate above 440 °C, while PT6 evaporates at 240 °C. The synthesized m-PCMs lost only 0.6% of their mass after heating at 40 °C for 8 days.

Afsharpanah et al. (2022) [64] quantitatively investigated a miniature cuboid freezer unit with two rows of serpentine tubes and connecting plates. The effect in this ice bucket of dimensionless flow and geometrical factors on serpentine and extended surfaces were studied, namely the Reynolds number and corrected Stefan number for refrigerant flow, coil pitch/tank height (γ_1), coil spacing/tank width (γ_2), coil diameter/tank diagonal length (γ_3), plate area/maximum plate area (γ_4), and plate thickness/pipe diameter (γ_5). The charging process is tracked by a stored energy ratio that takes into account both sensible and potential energy storage. Larger values of γ_1, γ_2, γ_4, and γ_5 result in higher charging rates. Full surface thickness plates (γ_4 = 1 and γ_5 = 0.0081) increase the time-averaged charge rate by 18%.

Table 4 summarises previous studies on the utilisation of PCMs for cold chain applications, including the type of PCMs, studied parameters, and findings.

Table 4. A summary of studies on the utilisation of PCMs for cold chain applications.

Authors (Year) [Reference]	Configuration/Composition	Study Type	Studied Parameters	Highlighted Results/Findings
Song et al. (2019) [57]	Dodecane as PCM and expanded graphite (EG) as the skeleton.	Experimental and Numerical	Effect of adding EG to dodecane.	The thermal conductivity of the dodecane/EG mixture is fifteen times greater than that of the dodecane alone.
Xiaofeng and Xuelai (2020) [58]	PCM1: (*n*-octanoic acid–myristic acid composite) and PCM2: (potassium sorbate–water composite).	Experimental and Numerical	The temperature of the cold storage material.	The amount of time that the box spends cooling and the temperature that it maintains both fluctuate but always stay within the parameters of what is considered to be an acceptable range for the purpose of preserving the quality of perishable goods.
Liu et al. (2022) [59]	Brine phase change material gels (BPCMGs).	Experimental	Stored cold energy.	When the total amount of cold energy stored is 691,800 J, the cold storage durations for aquatic goods and biological samples reach a maximum of 21.44 h and 16.37 h, respectively.
Ma et al. (2022) [60]	Utilizing sodium dodecyl benzene sulfonate (SDBS), polyacrylamide (PAM), and guar gum (GG), as well as adding $MgCl_2$, nano-copper oxide (nano-CuO), and covalently modified hydroxylated multiwall carbon nanotubes (MWCNT-OH) were also employed.	Experimental	Effect of adding $MgCl_2$, MWCNT-OH, SDBS, PAM, and GG.	The highest thermal performance was achieved by the phase change system consisting of mannitol/$MgCl_2$@MWCNT-OH/PAM. This system's thermal conductivity of 0.685 W/m K rose by 18.16%, and the amount of time spent in cold storage was cut by 57.3%.
Lin et al. (2022) [61]	PCM is derived from sodium sulphate decahydrate with the addition of KCl and NH4Cl, carboxymethyl cellulose (CMC), and borax (B).	Experimental	Effect of adding KCl and NH_4Cl, CMC, and B to PCM.	Analyses of the composites' microstructure as well as their chemical structures revealed that the produced materials have high levels of chemical compatibility.
Chang et al. (2022) [62]	Microcapsules of poly (urea-formaldehyde) (UF), where *n*-tetradecane is used as core material and SDS as an emulsifier.	Experimental	Temperature and mass fraction of microcapsules.	Latent heat functional fluid thermal conductivity rises with temperature and decreases with microcapsule mass fraction. Temperature or microcapsule fraction enhances its viscosity.
Ikutegbe et al. (2022) [63]	Microencapsulated PCM (m-PCM).	Experimental	Polymerisation time and optimum core–shell mass ratio.	Above 440 °C, the microcapsules began to decompose, whereas PT6 began to entirely evaporate at 240 °C. After 30 days of heating at 40 °C, the synthesised m-PCMs lost just 0.6% of their initial mass, which stabilized after 8 days of heating at that temperature.
Afsharpanah et al. (2022) [64]	A small ice container unit in the form of a cuboid, with two rows of serpentine tubes and connecting plates.	Numerical	The ratio of the serpentine tube pitch length to the container height (γ_1), the ratio of the serpentine tube row distance to the container width (γ_2), the ratio of the serpentine tube diameter to the container diagonal length (γ_3), the ratio of the plate area to the maximum plate area (γ_4), and the ratio of the plate thickness to the tube diameter (γ_5).	Enhanced charging rates are the result of higher values for γ_1, γ_2, γ_4, and γ_5 and lower values for γ_3. It was also discovered that using full-thickness plates (with a γ_4 value of 1 and a γ_5 value of 0.0081) results in an 18% boost in the time-averaged charging rate.

Regarding the information summarized in Table 4, one study indicates that the combination of dodecane and EG has a thermal conductivity that is fifteen times larger than that of dodecane alone. Additionally, the thermal conductivity of latent heat functional fluids upsurges with temperature and declines with microcapsule mass fraction. Further, the phase change system composed of mannitol/$MgCl_2$@MWCNT-OH/PAM produced the maximum thermal efficiency.

3.5. Other Applications

A comprehensive evaluation of the conducted studies published between 2016–2022 that investigated the utilisation of PCMs in other applications of CTES are detailed in the next sections.

In Dublin, Ireland, Browne et al. (2016) [65] described a revolutionary photovoltaic (PV), thermodynamic (T), and PCM system for generating electricity, storing heat, and preheating water in the open air. Thermo-syphonic flow removes heat from a heat exchanger embedded in PCM, and the system design combines a PV module with a thermal collector to achieve this. We compared the system's efficiency to three different scenarios: (a) with no PV module (PCM), (b) with no heat exchanger (HEX) and no PV module (PCM), and (c) with just the PV module (alone). It was shown that the water temperature was roughly 5.5 °C higher than in a PV/T system without PCM. It has been shown that PCMs are an efficient heat storage mechanism for use in PV/T systems.

Hussain et al. (2017) [66] investigated eutectic (oleic and capric) latent heat storage materials for refrigeration. Fabrication of highly porous activated carbon (AC) nano-sheets was performed to obtain improved thermo-physical properties. Freezing/solidification, DSC, and thermal diffusion analysis showed improved thermo-physical properties. Figure 21 shows a linear increase in the heat transfer rate from 0.02 to 0.1 wt.% for the nano-dispersed PCM, with a maximum time saving of 54% compared to the pure eutectic material. The thermal conductivities of pure PCM were 0.194 W/m K (liquid) and 0.201 W/m K (solid); 0.1 wt.% nano-dispersed PCM improved the value by 55%. The high nucleation rate eliminates PCM super-cooling at 0.1 wt.% AC in the base fluid.

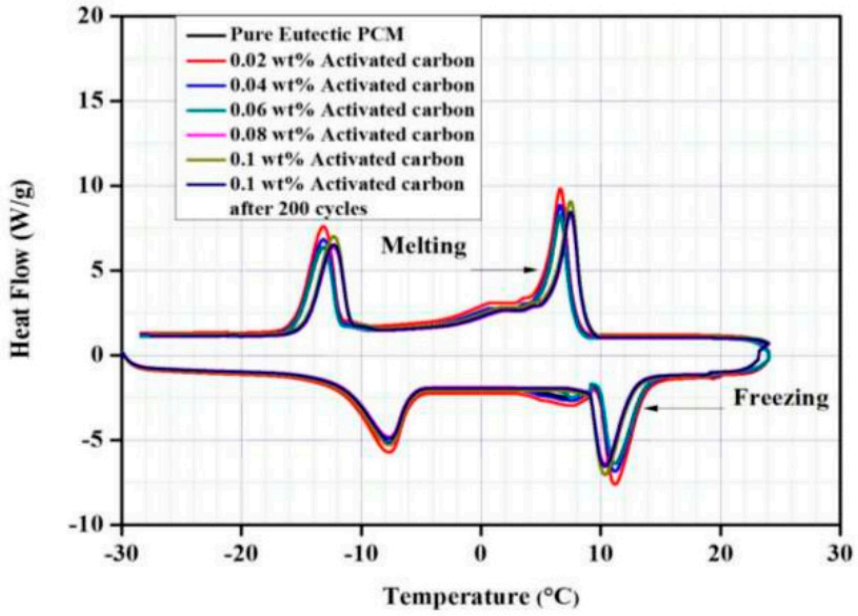

Figure 21. DSC analysis of pure and nano-enhanced eutectic PCMs [66].

Sze et al. (2017) [67] investigated a non-eutectic PCM, an aqueous solution of ethylene glycol and ethanol, to determine its potential for high-value refrigeration applications. Differential scanning calorimetry and thermal response measurements were used to characterize aqueous solutions of different concentrations. These experiments were performed

on bulk PCM. PCMs can be stored at a wide range of temperatures without phase separation problems. As shown in Figure 22, graphene oxide (GO) powder was used in the formulation at a concentration of 1 wt.% as a stabilizing nano-filler to improve thermal conductivity and reduce super-cooling levels.

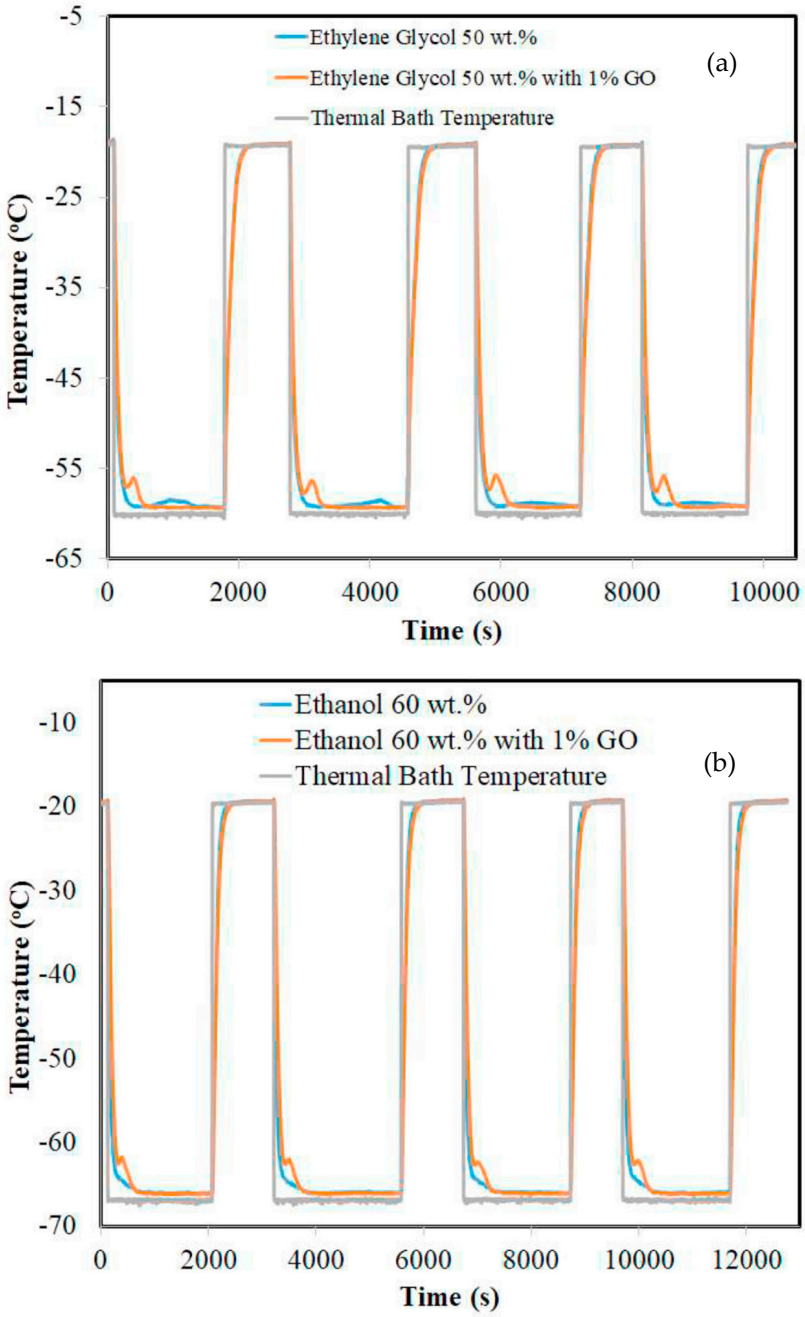

Figure 22. Thermal response measurements of aqueous ethylene glycol at: (**a**) 50 wt.% with and without 1% GO and (**b**) 60 wt.% with and without 1% GO [67].

A reused energy harvesting device was invented and created by Yu et al. (2018) [68] by integrating two PCMs (PEG and 1-TD) with N- and P-type semiconductors. Due to the differing phase transition temperatures between PEG and 1-TD, a temperature difference between the semiconductors' two sides was produced during both the heating and cooling processes. Graphene nano-platelet (GNP)-loaded graphene aerogel was employed as a supporting material to stop the leaking of PCMs. Utilising the output electric energy, a light bulb with a LED was illuminated after measuring the electric current. To help people

comprehend the energy harvesting system, the thermo-electric energy of the device was also numerically simulated. In both the heating and cooling processes, the maximum harvesting current was 10 mA, and the harvesting field was kept for 1900 s and 850 s, respectively. A finite element method (FEM) was used to predict the temperature variation and the consequent electric current with reference to time.

Huang et al. (2019) [69] mixed different concentrations of EG with water to produce PCMs with different freezing points. Then, 0.0625, 0.125, 0.25, and 0.5% MCNTs were added to each EG–water-based liquid. The latent heats of 15–30% EG–water-based fluids were 160, 141, 102, and 85.5 J/g, and the melting points were −12.2, −15.7, −22.1, and −25.4 °C, respectively. A moderate amount of MCNT has a negligible effect on the latent heat and melting point. The MCNT content in the EG–water-based fluid increases thermal conductivity. The thermal conductivity of solid samples increased more than liquid samples. In the 0.5% MCNT sample, the thermal conductivity of the solid is twice that of the liquid.

Talukdar et al. (2019) [70] studied PCM as a thermal backup system for solar cold storage during peak electricity demand or when there is no sun. The latent heat thermal energy storage (LHTES) unit (PCM pack) acts as a heat exchanger and consists of evaporator tubes and rectangular metal fins that facilitate heat transfer during PCM phase shifting. Evaporators with 5, 8, 10, and 12 longitudinal aluminium fins and no fins within the PCM package were examined. ANSYS Fluent 15.0 solidification and melting models use enthalpy porosity to create 3D simulation models. Figure 23 shows that a PCM package with more fins freezes faster and stores more energy after melting.

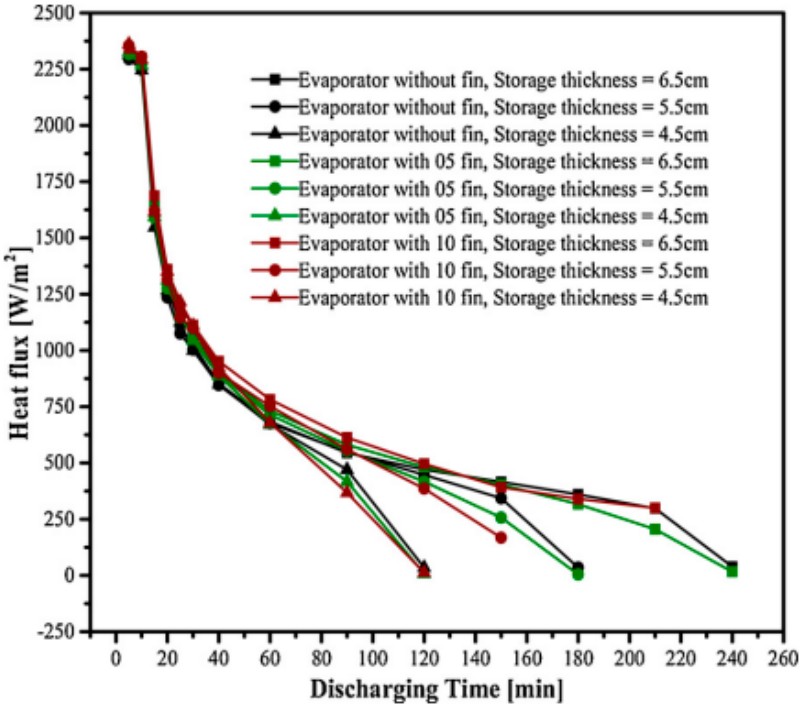

Figure 23. Heat flux vs time graph showing effect of variation of thickness of PCM pack and number of fins used during melting [70].

Dhivya et al. (2019) [71] investigated the influence of weight percentage of nanoparticles added to PCMs for the possible remedy of low thermal conductivity. They created microcapsules of silver (Ag)-doped ZnO nanoparticles distributed in eutectic PCM containing oleic/myristic acid. In the eutectic mixture, Ag-doped ZnO nanoparticles were introduced in mass fractions of 0.05 wt.%, 0.1 wt.%, 0.15 wt.%, and 0.2 wt.%. The results showed that thermal conductivity rose by 2.78%, 27.17%, 37.56%, and 48.62%, respectively, and microencapsulated eutectic PCMs can be recommended as a suitable core material for low-temperature latent heat thermal energy storage applications.

Zou et al. (2020) [72] reported the effect of expanded graphite (EG) size on the thermal properties of polycrystalline graphite (PCM). Three different sizes of EG (50, 80, and 100 mesh) were selected for PCM as support material for the fabrication of their respective composite CPCMs. The results showed that the effect of EG-50 on the shape stability and adsorption rate of modified $CaCl_2.6H_2O$-PCM was significantly better than that of EG-80 and EG100. Each of the three different forms of CPCM has a slightly lower temperature compared to the melting temperature T_m of the original modified $CaCl_2.6H_2O$ PCM. The T_m changes of assembled PCMs may be caused by EG-induced alignment of modified $CaCl_2.6H_2O$-PCMs around EGs, which may affect local steric hindrance. This transition may occur due to EG-induced targeting. Therefore, of the three different EG types, the EG-50 is the one with the largest pore size, followed by EG-80 and then EG-100. This results in a CPCM with a lower melting temperature, as shown in Figure 24.

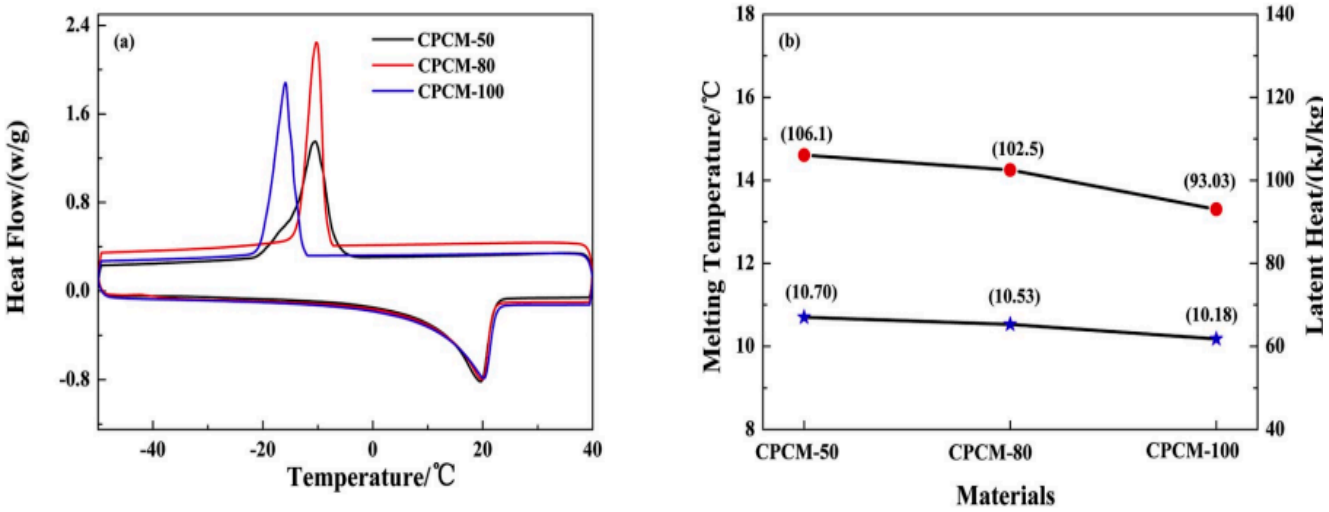

Figure 24. (**a**) DSC curves and (**b**) the corresponding thermal properties of three kinds of modified $CaCl_2$ $6H_2O$/EG CPCMs [72].

Borri et al. (2020) [73] established a cylindrical experimental setup to obtain sub-zero thermal distribution of PCMs. Deionized water (ice) was used to calibrate and validate a 1D model, as shown in Figure 25. Sodium chloride, ethylene glycol, and decane were tested as sub-zero PCMs. The numerical results for hydrous alcohol were the most consistent with the test. The experimental and mathematical results for paraffin and aqueous sodium chloride are different. Figure 26 shows that this difference is due to natural convection during melting and sub-cooling during solidification.

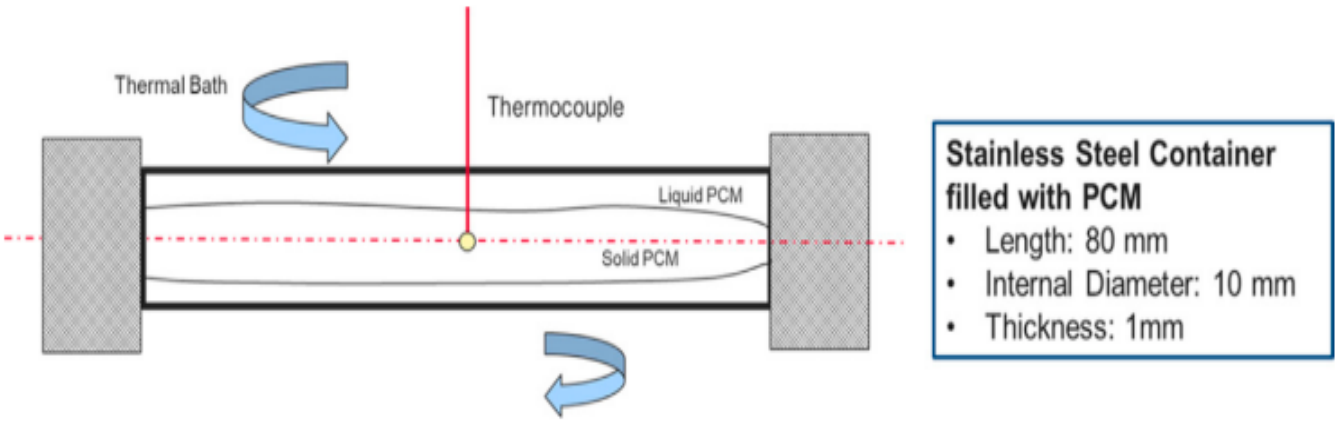

Figure 25. A scheme of the PCM container and main dimensions [73].

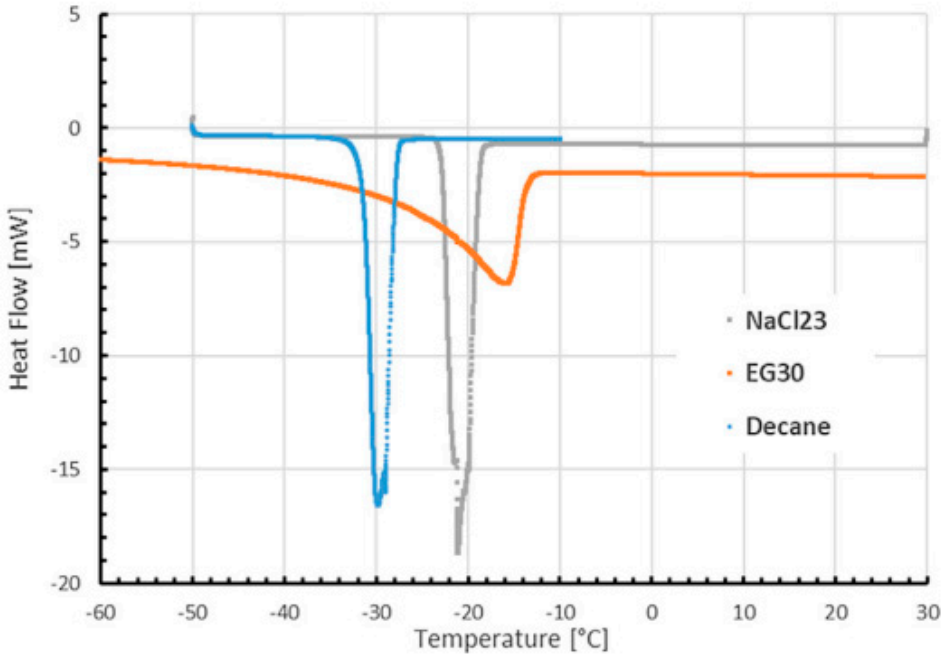

Figure 26. Heat Flow of the different PCMs measured with DSC [73].

Rakkappan et al. (2021) [74] prepared 1-decanol-expanded graphite composites (CPCM) as a substitute for ice in a cold thermal energy storage system (CTESS). CPCMs are macro-packaged in 42, 51, and 64 mm spherical shells (S.E.s) and tested at various wall temperatures (Tw) for charge (0, −3, and −6 °C) and discharge (10, 13, and 16 °C), as shown in Figures 27 and 28. CPCM can store latent heat at a higher wall temperature (−3 °C) than ice. CPCM-filled 51 mm S.E. 1-decanol freezes 85.37% faster than PCM-filled S.E. at −6 °C. The optimal wall temperatures for charging and discharging are −3 and 13 °C, respectively, as shown in Figure 29. Diameter affects loading and unloading. With a 51 mm S.E. CPCM, the PCM requires 81.27% and 76.45% less time to store (Tw = −3 °C) and recover (Tw = 16 °C) a given amount of energy, respectively.

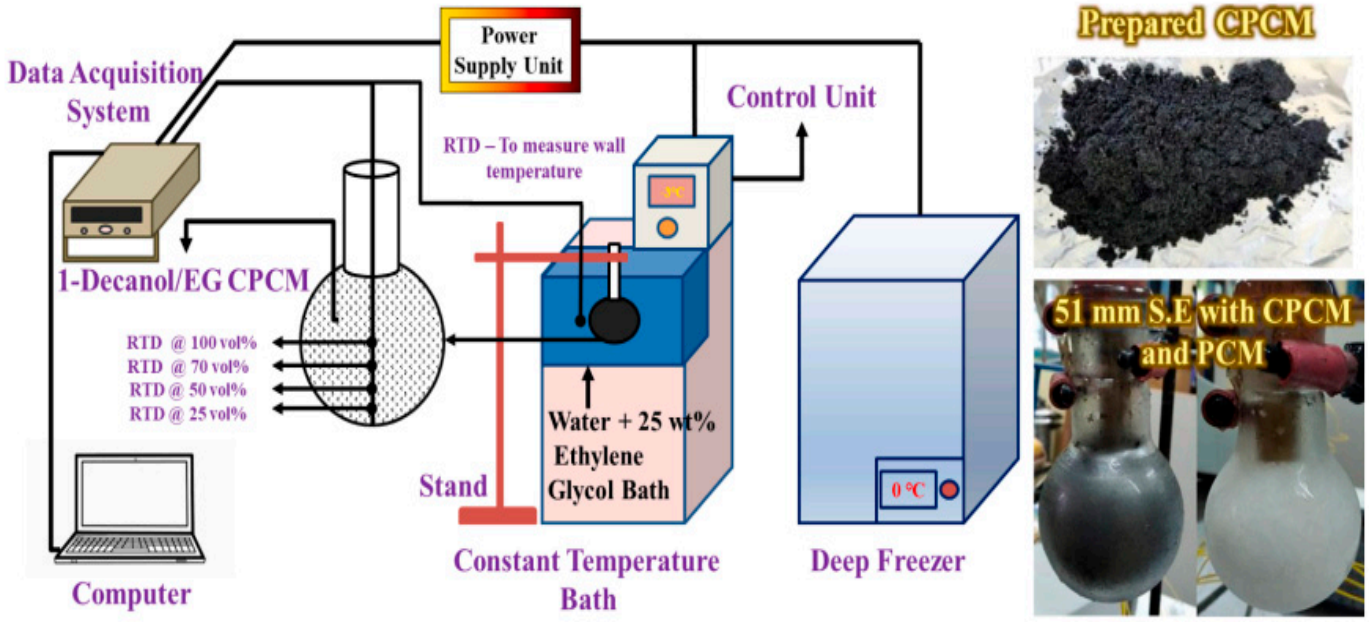

Figure 27. Experimental setup used to investigate the energy storage characteristics [74].

Figure 28. Macroscopic pictures of the prepared CPCM [74].

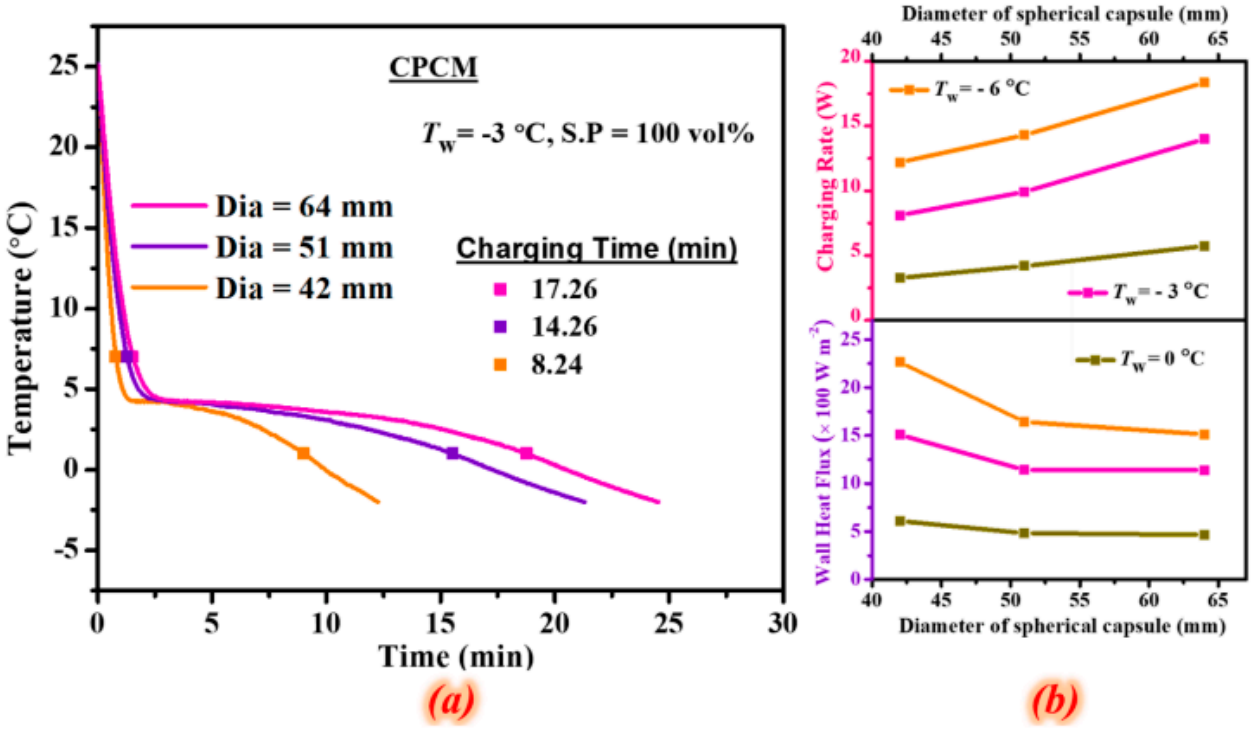

Figure 29. (**a**) Effect of diameter on Charging behaviour of CPCM and (**b**) Charging rate and wall heat flux realized in various diameters at different wall temperatures [74].

Nie et al. (2021) [75] investigated a portable PCM box for cold chain transportation presentations. As shown in Figure 30, a composite PCM of graphene, fumed silica, and paraffin (RT 5) was used in this study. Portable boxes with composite PCMs required the construction of an experimental setup so that the charging time, cooling time, and power efficiency of the portable boxes could be compared. The findings indicated that the composite PCMs exhibited high cyclability and chemical stability. PCM leakage can be stopped by adding 4 wt.% fumed silica to the mixture. When graphene was added to the mixture at 1% by weight, the thermal conductivity of the composite increased by 55.4%. Box loading time is reduced by 6.25% when using the composite PCM. The onset of melting and the freezing point of the composite PCM almost exactly matches those of pure PCMs. As shown in Figure 31, this shows that the incorporation of graphene and fumed silica into the composite has little effect on the temperature at which the phase transition occurs.

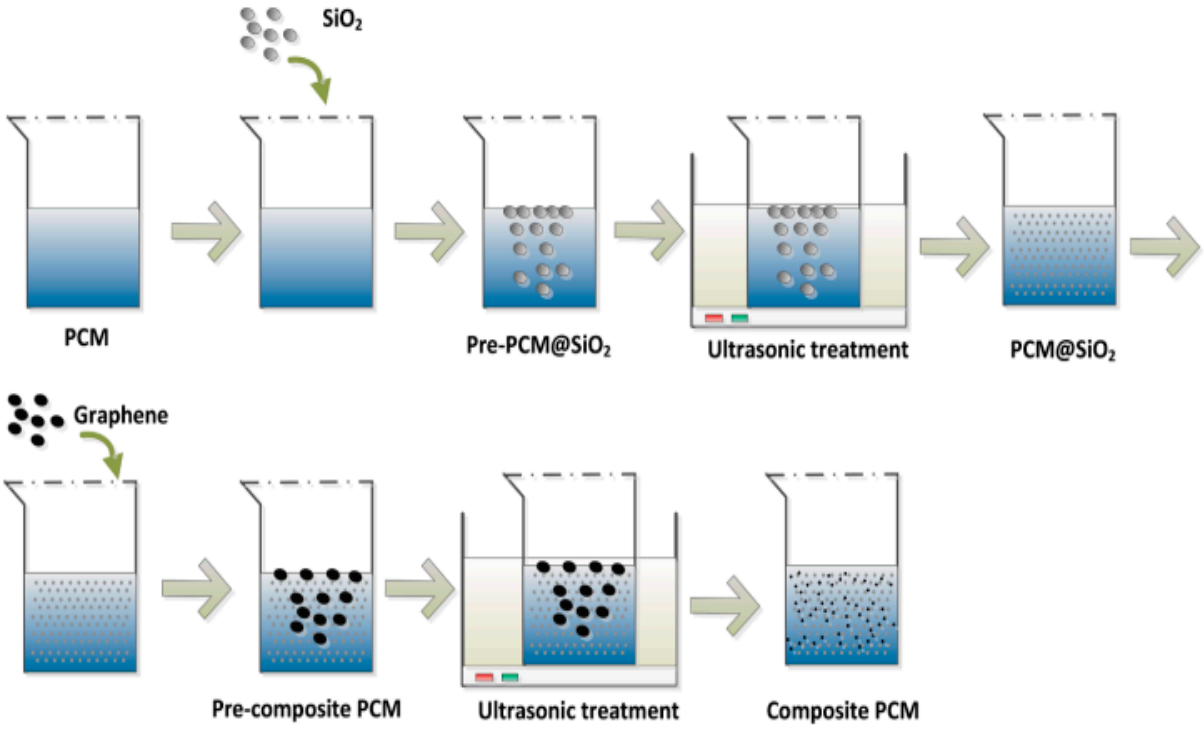

Figure 30. A schematic diagram of the formulation of the composite PCM [75].

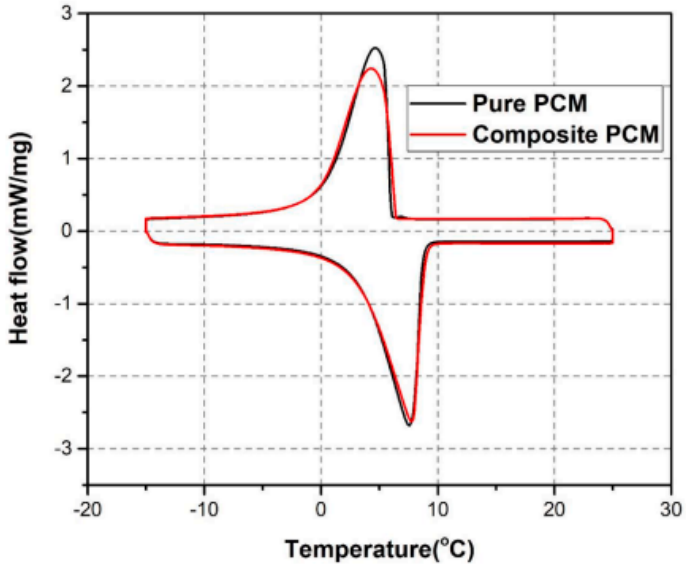

Figure 31. DSC curves of different PCMs [75].

Tafone et al. (2021) [76] modelled and tested a low-temperature high-grade cold storage (HGCS) fixed bed filled with PCM. A 1D transient model that simulates HGCS charging and discharging was developed. Numerical results show that the utilisation of PCM in the HGCS alleviates the thermocline effect exhibited in the sensible heat (SH) configuration, resulting in (a) a longer discharge phase and (b) a lower unit consumption with a thermal buffering phenomenon triggered by the phase transition process. The configuration is guaranteed compared to the SH configuration (0.272 vs. 0.330 kWhe/kgLA). Figure 32 shows the various billing processes. The initial fixed bed and HTF inlet temperatures were 25 °C and −155.8 °C, respectively. HTF and particle temperature trends are comparable but slightly biased.

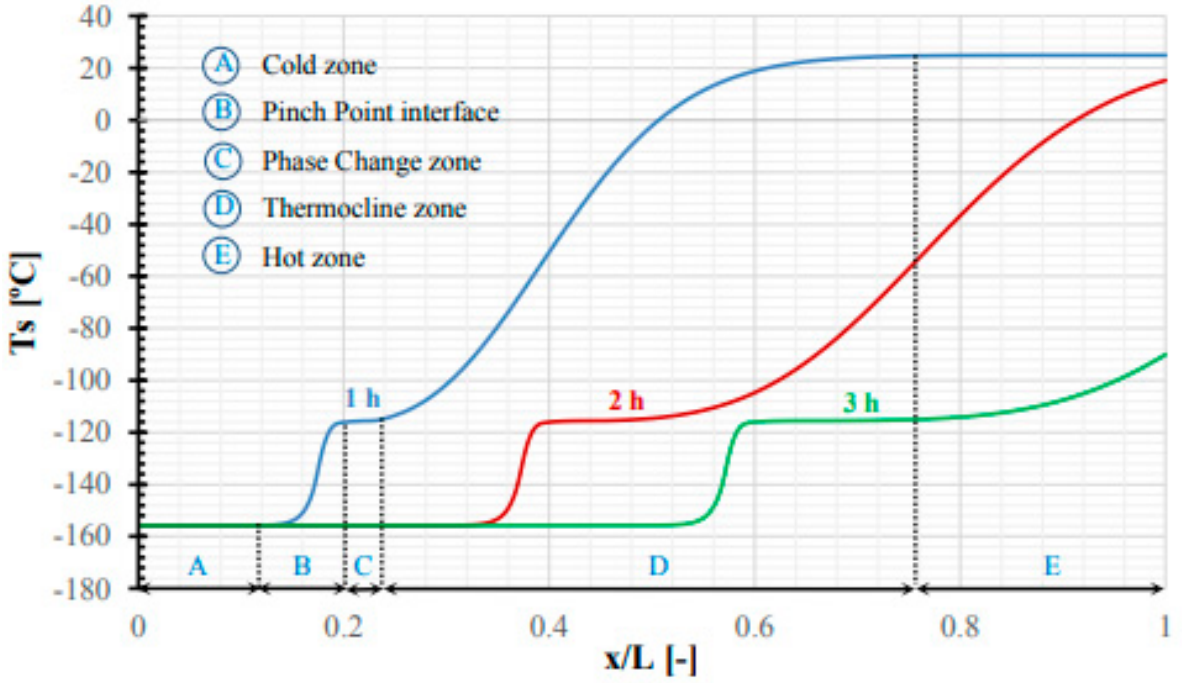

Figure 32. The bed temperature profile of PCM configuration at different time steps (1 h, 2 h, 3 h) [76].

Rezaei et al. (2021) [77] introduced an innovative heating, ventilation, and air conditioning (HVAC) system to address the negative effects of conventional HVAC systems on the driving range of electric vehicles. A heat pump and an outside heat exchanger that runs parallel to a shell-and-tube heat exchanger that employs PCM comprised the HVAC system. This heat exchanger may temporarily function as both the cycle's condenser and evaporator. N-hexadecane serves as the PCM in the shell while R134a serves as the refrigerant in the tubes. When the PCM's specific melting point is within the safe working range, the system's overall power consumption, as well as the compressor's, are lowered. A copper foam is used to make up for PCM's low heat conductivity. The results showed that the proposed system increased the vehicle range by 19% at 10 °C and by 11% at 0 °C when compared to conventional heat pump systems.

Sarafoji et al. (2022) [78] proposed a new PCM using a 53:47 wt.% lauryl alcohol–capric acid (LA–CA) binary mixture; 0.25 wt.% TiO_2 and CuO nanoparticles are added to the PCM mix. Chemical and thermal analysis of the LA–CA mixture demonstrated the stability of the mixture for TES. The melting temperature of the PCM mixture was 9.57 °C and the latent heat was 159.4 J/g. The thermal conductivity of the LA–CA/CuO PCM is increased by 17.56%, the melting temperature is 8.7 °C, and the latent heat is 159.1 J/g. The LA–CA/CuO PCM exhibited high thermal and chemical stability after 1000 cycles.

Wang et al. (2022) [79] investigated the heat transfer, energy conversion, and efficiency of a novel tetrabutylammonium bromide (TBAB) hydrate cold storage system during cold discharge. The process includes a gas turbulence device and a hydrate coil heat exchanger. The heat exchange balance during cold charge and discharge buffers the storage temperature. Forced convection of gas turbulence improves cold discharge capability and reduces discharge time by a factor of three. Increased flow and lower cold discharge temperature increase cold discharge capacity. With different settings, the cooling efficiency is 83%.

Mousavi et al. (2022) [80] evaluated a liquid air energy storage (LAES) system from a thermodynamic and economic perspective. The system uses a packed bed thermal energy storage device (PBTES) consisting of three layers of PCM. Due to the transient nature of PBTES, dynamic modelling was used to study the efficacy of the system. This was performed to ensure correct results. At peak, the proposed LAES system consumes

4.42 MWh of energy to compress the air but generates only 1.8 MWh of electricity for use. The system's liquid production, the mass flow of liquid air, the specific work performed by the compressor, and the cryogenic turbine all change with each cycle. This is due to the dynamic behaviour of the system. After about 22 cycles, the system entered a steady state with an overall efficiency of 42.5%, and the system performance degraded by about 5.9% compared to ideal cycles due to transient behaviour.

Wu et al. (2022) [81] proposed and numerically investigated a novel latent heat thermal energy storage (LHTES) device with different heating and cooling sources. The LHTES devices include symmetrical and staggered configurations with side- and bottom-heated LHTES devices, as well as newer LHTES devices with discrete heating and cooling sources. The findings show that the discrete configuration of the sources greatly enhances the additional conduction effects and natural convection in the side-heated LHTES unit. The heat storage and release cycle of the symmetrical arrangement of side heating is shortened by 49.9%, the heat preservation time is advanced by 46.6%, the heat preservation liquid rate is increased by 4.2%, and the heat transfer rate is increased by 22.3%. These are the most important improvements. The increase in performance due to the discrete source placement of the LHTES device through floor heating is not discernible.

Laouer et al. (2022) [82] investigated the performance of two techniques to improve heat transfer, namely adding fins and mixing nanoparticles (Cu and Al_2O_3) to improve the melting process of PCM (water) in inclined rectangular shells, used as a refrigeration system. PCM phase transition and heat transfer modelling was conducted using in-house-developed code based on the Lattice Boltzmann method. The code was validated with experimental and numerical data within the published literature. The evaluation of the reinforcement effect is mainly based on the number of ribs, the ratio of rib length to nanoparticle size (W/H), and the volume percentage of nanoparticles (ϕ). The melting rate at a rib length ratio of W/H = 0.75 is almost twice that at W/H = 0.25. Furthermore, the loading of nanoparticles leads to a further acceleration of the melting rate. Using three fins and a nanoparticle concentration of ϕ = 6 vol.%, the melting rate can be increased to the maximum potential, resulting in a 33.5% reduction in the time required for the overall melting process. By increasing the aspect ratio of the fins, more thermal energy can be stored, reducing the time required for the melting process by up to 64%.

Feng et al. (2022) [83] tested a finned latent heat storage device. Modified expanded graphite (MEG) is used to expand the thermal properties of water on the fin side of the heat exchanger. Experimental studies of the charge–discharge process show that a system loaded with 90% water/MEG has 80% of the cooling capacity of pure water but only 69% of the cooling time and 15.9% more power than water. The 90% water/MEG system performs two charge and discharge cycles. A mathematical model was built and authenticated to examine the effect of phase transition behaviour and structure size on system performance. The fin spacing of the heat exchanger has no effect on cold storage, but the pipe spacing does.

Liu et al. (2022) [84] developed a ground-breaking phase change cold storage unit (PCCSU) as a mobile refrigeration unit for transporting refrigerated vehicles to improve the efficiency of room temperature control. The PCCSU was placed at the front of a thermally shielded internal compartment and charged using a refrigeration system during non-operational hours. The cold thermal energy of the PCCSU cooled the chamber. The experiment's findings were obtained at a variety of cold temperatures, with accompanying energy expenditures and transportation-related dangers. The results showed that the efficiency of the temperature regulation system was significantly improved when the suggested PCCSU was installed in the thermally insulated space. In comparison to conventional PCM refrigeration systems, it also permits a wider variety of temperature configurations. The average air temperature of the inner compartment could be preserved at 12.3 °C for 16.6 h, 14.5 °C for 14.7 h, and 16.5 °C for 10 h in the hot summer with an average ambient temperature of 29 °C.

Table 5 summarises previous studies on the utilisation of PCMs for cooling in different applications, including the type of PCMs, studied parameters, and findings.

Table 5. A summary of studies on the utilisation of PCMs for cooling in different applications.

Authors (Year) [Reference]	Configuration/Composition	Study type	Studied Parameters	Highlighted Results/Findings
Browne et al. (2016) [65]	Novel PV/T/PCM system.	Experimental	Influence of using PCM.	Water temperature was roughly 5.5 °C higher than that of a PV/T system without PCM.
Hussain et al. (2017) [66]	PCM in a base fluid that contains 0.1 weight percent of activated carbon.	Experimental	Effect of adding highly porous activated carbon (AC) nano-sheets.	When compared to pure eutectic, the highest time savings was 54%, and the heat transfer rate increased linearly from 0.02 wt.% to 0.1 wt.% for nano-dispersed PCM.
Sze et al. (2017) [67]	Aqueous solutions of ethylene glycol and ethanol, with a stable nano-filler consisting of graphene oxide powder at a concentration of 1% by weight.	Experimental	Effect of adding graphene oxide on super-cooling, melting, and latent heat of fusion.	After adding 1 wt.% graphene oxide, super-cooling degrees for 49.5 wt.% ethylene glycol dropped by 61% from 9 °C to 3 °C. Melt beginning and peak temperatures are now −53 °C and −36 °C, respectively. The latent heat of fusions was reduced by 12% for 50% ethylene glycol and 6% for 60% ethanol.
Yu et al. (2018) [68]	An energy harvesting system was developed by integrating two PCMs (PEG and 1-TD) with N- and P-type semiconductor while utilising graphene nano-platelets as a supporter and promoting the shape stability.	Experimental and Numerical	The electric current measured from the energy harvesting device was studied for variable environmental temperatures.	The maximum harvesting current was 10 mA for both the heating and cooling processes, and the harvesting fields were maintained for 1900 and 850 s, respectively.
Huang et al. (2019) [69]	After adding EG of varying concentrations to the water, MCNT at concentrations of 0.0625%, 0.125%, 0.25%, and 0.5% was then distributed into each of the EG-water-based fluids.	Experimental	EG concentration and particle volume fraction.	Due to the very low overall concentration of MCNT, the addition of MCNT has a negligible impact on the latent heat and melting point of the material. Additionally, the quantity of MCNT that is concentrated in EG–water-based fluids causes a rise in the thermal conductivity of the fluids.
Talukdar et al. (2019) [70]	PCM pack occupied by PCM acts as a heat exchanger.	Experimental and Numerical	Effect of longitudinal aluminium fins inside the PCM pack and thickness of PCM pack.	The PCM pack with a thickness of 6.5 cm and a greater number of fins was found to have a larger energy storage capacity as well as a higher heat flow during the melting process.
Dhivya et al. [71]	Microcapsules of silver (Ag)-doped ZnO nanoparticles with different mass fractions distributed in eutectic PCM containing oleic/myristic acid.	Experimental	Explore the effect of the weight percentage of nanoparticles added to PCMs for improving the thermal conductivity.	The thermal conductivity increases by 2.78%, 27.17%, 37.56%, and 48.62%, due to adding 0.05 wt.%, 0.1 wt.%, 0.15 wt.%, and 0.2 wt.%, respectively.
Zou et al. (2020) [72]	EG added to $CaCl_2$ $6H_2O$ PCM.	Experimental	Mass fraction and size of EG.	The impact of EG-50 in maintaining the form was deemed to be superior to that of EG80 and EG-100. The disparity in thermal performances of CPCMs was brought on by the dissimilarities in the sizes of their EG components.
Borri et al. (2020) [73]	Aqueous sodium chloride, aqueous ethylene glycol, and decane.	Experimental and Numerical	Type of PCM.	According to the trials, aqueous alcohol showed the greatest level of agreement.
Rakkappan et al. (2021) [74]	Composite made of graphite that has been expanded with 1-decanol (CPCM).	Experimental	Macro-encapsulated diameter and wall temperature.	The optimal wall temperature for charging is determined to be −3 °C, whereas the optimal wall temperature for discharging is found to be 13 °C. Both the charging and discharging rates are higher with larger diameters.

Table 5. *Cont.*

Authors (Year) [Reference]	Configuration/Composition	Study type	Studied Parameters	Highlighted Results/Findings
Nie et al. (2021) [75]	Paraffin-based PCM (RT 5), fumed silica, and graphene.	Experimental	wt.% of graphene and fumed silica.	The composite's heat conductivity rose by 55.4% when graphene at a weight fraction of 1% was added to it. The PCM leakage was able to be stopped with the addition of 4 weight percent of fumed silica. By using silica and graphene, one may improve the nucleation process of phase change kinetics and lower the amount of PCM super-cooling that occurs.
Tafone et al. (2021) [76]	Novel cryogenic HGCS packed bed filled with PCM.	Experimental and Numerical	Effect of introducing a PCM in the HGCS.	The incorporation of a PCM into the HGCS helps to reduce the thermocline effect that is seen in the SH configuration. This results in the following advantages over SH design: a longer discharge phase and lower specific consumption (0.272 kWhe/kgLA as opposed to 0.330 kWhe/kgLA).
Rezaei et al. (2021) [77]	A novel HVAC system made up of a heat pump and an outside heat exchanger that runs parallel to a shell-and-tube heat exchanger that uses N-hexadecane PCM and R134a as the refrigerant in the tubes.	Experimental and Numerical	Effect of the specific melting point of N-hexadecane PCM on compressor's power consumption and overall performance of the vehicle	In comparison to traditional heat pump systems, the system that is suggested enhanced the vehicle's range by 19% at 10 °C and by 11% at 0 °C, according to the results.
Sarafoji et al. (2022) [78]	In the beginning, the PCM mixture comprised a binary mixture of lauryl alcohol and capric acid (LA–CA) with 53:47 wt.%; afterwards, TiO_2 and CuO nanoparticles were added to the mixture at 0.25 wt.%.	Experimental	Effect of weight % lauryl alcohol–capric acid and the TiO_2 and CuO nanoparticles.	The thermal conductivity of the suggested LA–CA/CuO PCM is increased by 17.56% with the incorporation of nanoparticles. The PCM has a melting temperature of 8.7 °C and a latent heat of 159.1 J/g. Even after 1000 cycles, the thermal and chemical stability of the suggested LA–CA/CuO PCM remains outstanding. This is due to the PCM's high copper content.
Wang et al. (2022) [79]	Tetrabutylammonium bromide (TBAB) hydrate cold storage system.	Experimental	Gas disturbance, cold charge temperature, and flow rate.	Gas disturbance forced convection, increased cold discharge capacity, and shortened discharge time by a factor of three. Increasing flow rate and reducing cold charge temperature enhanced cold discharge capacity. Under diverse settings, cold discharge efficiency was 83%.
Mousavi et al. (2022) [80]	System for the storage of liquid air energy (LAES), which makes use of a packed bed for thermal energy storage (PBTES).	Numerical	Cycles of the system.	The system with a general efficacy of 42.5% reaches the equilibrium state after about 22 cycles, and transient behaviour causes the performance of the system to decline by around 5.9% in comparison to the optimum cycle.
Wu et al. (2022) [81]	LHTES unit that has separate heat and cold sources, including symmetrical and staggered layouts with side-heated and bottom-heated LHTES applications.	Numerical	Arrangements of heat and cold sources.	The side-heated and symmetrical arrangement reduced the heat storage and release cycle by 49.9%, advanced the steady-state period by 46.6%, raised the steady-state liquid percentage by 4.2%, and enhanced the heat transfer rate by 22.3%. The separate source configuration did not increase bottom-heated LHTES performance.

Table 5. *Cont.*

Authors (Year) [Reference]	Configuration/Composition	Study type	Studied Parameters	Highlighted Results/Findings
Laouer et al. (2022) [82]	Enhancing the melting process of PCM (water) in an inclined rectangular container by adding fins and hybrid nanoparticles made of copper and aluminium oxide.	Numerical	Number of fins, fin length ratio, and nanoparticle volume fraction.	When compared to a ratio of W/H equal to 0.25, the rate of melting is about two times greater when the fin length ratio is W/H = 0.75. In the case of three fins and a nanoparticle concentration of ϕ= 6 vol.%, the melting rate may be increased to its maximum potential, resulting in a time reduction in the full melting process by 33.5%.
Feng et al. (2022) [83]	Water and modified expanded graphite (MEG).	Experimental and Numerical	Heat exchanger fin spacing and wt.% water/MEG.	Heat exchanger fin spacing did not affect the cold energy storage unit, but tube pass spacing did. The system's cooling capacity, cooling duration, and average power were 80.8%, 69.7%, and 15.9% greater than those of pure water, respectively.
Liu et al. (2022) [84]	A ground-breaking phase change cold storage unit (PCCSU) was developed as a mobile refrigeration unit for the transport of refrigerated vehicles	Experimental		In a hot summer with an average ambient temperature of 29 °C, the average air temperature of the inner compartment could be maintained at 12.3 °C for 16.6 h, 14.5 °C for 14.7 h, and 16.5 °C for 10 h.

To summarise Table 5, it was shown that tube pass spacing, not heat exchanger fin spacing, had an impact on the cold energy storage unit investigated in one study. Additionally, it was found that a PCM pack with a thickness of 6.5 cm and more fins had a stronger heat flow during the melting process as well as a greater energy storage capacity. Additionally, the heat transfer rate rose linearly for a nano-dispersed PCM from 0.02 wt.% to 0.1 wt.%, with the largest time savings of 54% when compared to a pure eutectic PMC.

4. Critical Evaluation on Utilising PCMs in Different CTES Applications and Nominal Improvements

This section focuses on conducting a critical evaluation review on deploying PCMs in different sectors of CTES. Apparently, eutectic, organic, and inorganic PCMs were intensively deployed for various applications of CTES. However, the popularity of their usage is quite linked to their thermal and physical characteristics in addition to a number of specific requirements and considerations. The following points demonstrate some conceptual facts drawn from the covered studies and associated studies:

- Organic, inorganic, and eutectic PCMs (binary and ternary) all have benefits and are used in CTES applications. Basically, the decision between them is influenced by criteria such as the needed temperature range, heat transfer efficiency, cost considerations, safety regulations, and the unique needs of the application. However, it should be noted that eutectic PCMs provide optimum advantages that make them suited for a wide range of applications in a variety of applications. For instance, eutectic PCMs have a stable and clearly stated melting point, allowing them to move through a sudden phase change at a given temperature. This property assures consistent and reliable thermal behaviour, making them perfect for specific applications requiring exact temperature control. Furthermore, eutectic PCMs possess considerable latent heat capacities, which means they can store and release a large quantity of thermal energy during the phase transition process. This characteristic enables them to deliver optimal temperature regulation and thermal buffering by effectively storing thermal energy. Compared to organic and inorganic PCMs, eutectic PCMs have higher thermal conductivity. This allows for faster heat transmission during the phase transition process, making them suited for applications that demand rapid heating or cooling cycles. Eutectic PCMs have been designed to sustain several phase change cycles without

deterioration. Their capacity to withstand multiple melting and solidification cycles without deterioration in performance makes them suitable for long-term applications. These characteristics also contribute to their popularity and adaptability. This can contribute to a diverse selection of sectors employing eutectic PCMs including building and construction, energy storage, HVAC systems, thermal regulation in electronics, cold chain management, and thermal comfort enhancement in clothing and textiles. New eutectic PCM formulations and their uses may arise as research and technology advance in the future;

- Incorporating eutectic phase transition materials into wall boards, concrete, gypsum, flooring, and other building materials reduces energy expenditure while increasing thermal comfort. Many examples of successful implementation of PCMs for cold storage in buildings were described in [37–43]. Apparently, macro-encapsulation provides an effective, secure, and straightforward means of using eutectic PCM, among numerous integration approaches, and its potential uses have received a lot of attention in recent years;
- Because organic eutectic PCMs are often non-toxic, non-corrosive, less chemically reacted, pose fewer environmental concerns, and have customized melting temperature and enthalpy, they are suitable for thermal energy storage in electronics and structures such as portable cooling units and temperature-controlled packaging. However, it should be noted that each organic eutectic PMC has a specific melting point and latent melting enthalpy and, therefore, it would suit a unique application only [85];
- When a specific, narrow temperature range must be implemented for an application, eutectic PCMs are frequently preferred. Their fast phase change enables precise temperature control. Organic PCMs, on the other hand, may be preferable when a wider range of cooling temperatures is appropriate. However, eutectic PCMs have low heat conductivity and leakage during the phase transition, which severely limits their application. Therefore, advanced research was conducted to develop shape-stabilized composites in addition to enhancing their thermal conductivity. One plausible option was to add metallic nanoparticles and carbon-based materials of high thermal conductivity to eutectic PCMs in addition to mitigating the leaking of PCMs. Also, the dispersion of nanoparticles in specific mass fractions and an increase in the mass fraction of nanoparticles can significantly improve the heat transfer characteristics of eutectic PCMs, leading to a reduction in solidification and melting time. Other colleagues were focused on adding different conductive materials such as expanded graphite, carbon nanotube TiO_2, and ZnO. Detailed examples of the most advanced methods were elucidated by Veerakumar and Sreekumar (2015) [27], Dong et al. (2022) [43], Zheng et al. [44], Said and Hassan (2018) [46], Song et al. (2019) [57], Xiaofeng and Xuelai (2020) [58], and Hussain et al. [66]. Most importantly, the characteristics of higher thermal conductivity of eutectic PCMs compared to organic PCMs have allowed for faster heat transfer during the phase change process. In turn, this paved the way towards the implication of eutectic PCMs in several applications that necessitate rapid cooling or temperature stabilization.

5. Conclusions

This study reviewed the current research literature on the use of PCMs as latent heat energy storage strategies in different sectors of cold thermal energy storage systems. The review started by illustrating the classification, selection criteria, and performance testing and addressing the greatest challenges encountered with their utilisation in different applications of cold thermal energy storage. Second, for each aspect examined, the proposed studies fall into three distinct categories: experimental, numerical, and experimental and numerical studies. As a summary, five tables were prepared: the first table summarised the associated studies of PCMs for cold energy storage in buildings; the second table summarised the conducted studies using PCMs for air conditioning and refrigeration; the third table summarised the use of PCMs for cold chain applications; the fourth table summarised

the studies using PCMs for cold chain applications; and the fifth table summarised the studies using PCMs for cooling in other applications. Specifically, different experimental and numerical studies for cold energy storage applications were evaluated. Based on the thermal performance analysis included in each study examined and the evaluation of the results contained in Tables 1–5, it can be stated that eutectic PCMs are an appealing solution for a wide range of thermal management and energy storage applications due to their dependability, efficiency, and versatility. Furthermore, eutectic PCMs possess considerable latent heat capacities, which means they can store and release a large quantity of thermal energy during the phase transition process. Thus, it is not surprising to notice the wide applications of eutectic PCMs as they are useful for long-term applications due to their ability to resist numerous melting and solidification cycles without performance degradation. Further important conclusions related to the improvements made in the utilisation of PCMs in different applications of thermal energy storage systems can also be made in the following:

1. Cold storage in buildings: Smaller PCM ball diameter and faster chilled water flow rate increase freezing speed;
2. Air conditioning systems: Phase change cold storage has a capacity that is 1.5 times greater than ice cold storage and offers better overall performance. Also, when the inlet air temperature of the phase change material air conditioner is 35 °C, the PCM-equipped air conditioner outperforms the conventional unit by 14%, 13%, and 12%at inlet velocities of 0.96 m/s, 1.2 m/s, and 1.44 m/s, respectively;
3. Refrigeration systems: With three fins and a nanoparticle concentration of ϕ = 6 vol.%, the melting rate can be increased to its maximum potential, resulting in a 33.5% reduction in the time of the overall melting process;
4. Cold chain applications: As the temperature rises and the mass fraction of microcapsules increases, the thermal conductivity of the latent heat functional fluid drops. Furthermore, higher values of coil pitch/tank height, coil spacing/tank width, plate area/maximum plate area and plate thickness/pipe diameter result in higher charging rates. Full-thickness plates (plate area/maximum plate area = 1 and plate thickness/pipe diameter = 0.0081) increase the time-averaged charge rate by 18%;
5. Cold storage applications: Adding 4% fumed silica stops PCM leakage. Silica and graphene improve PCM nucleation and minimise super-cooling;
6. Finned heat exchanger: The cooling capacity, cooling time, and average performance of the system are 80.8%, 69.7% and 15.9% greater than those of pure water, respectively;
7. Solar cold storage: The PCM package with many fins has a larger energy storage capacity and a larger fusion heat flux.

6. Recommendations for Future Research Directions

The following recommendations can be drawn from the current review:

1. Increasing the heat storage density of PCMs is vital when developing a more efficient structure of cold chain transportation and refrigeration equipment;
2. It will be an interesting future research direction to study the phase transition behaviour of aqueous solutions including other forms of carbon nano-fillers;
3. In the context of cold thermal energy storage systems, it is important to study the thermal effects of many different radial configurations, geometries, initial temperatures, heat transfer fluid temperatures, and heat transfer coefficients;
4. Incorporating super-cooling and extending the prior approaches to various container forms and boundary circumstances are possible future advances;
5. A special focus is needed on the low charging rate and device design methodology for future commercial application;
6. It is rare to find an accessible paper on the subject of corrosion analysis of eutectic PCM containers. As a result, greater research into novel eutectic PCMs and corrosion studies of container materials is proposed.

Author Contributions: Conceptualization, F.L.R. and M.A.A.-O.; methodology, F.L.R., A.H., A.D., and A.H.; software, H.B.M.; validation, F.L.R., L.F.A.B., H.B.M., Z.A.A.R. and A.H.; formal analysis, M.A.A.-O. and L.F.A.B.; investigation, Z.A.A.R. and A.H., F.L.R.; resources, A.D. and A.H.; data curation, F.L.R., A.D., Z.A.A.R., H.A.H. and M.A.A.-O.; writing—original draft preparation, F.L.R., M.A.A.-O., A.D., L.F.A.B., H.B.M., A.H. and H.A.H.; writing—review and editing, F.L.R., M.A.A.-O., A.D., L.F.A.B., Z.A.A.R., A.H. and H.A.H.; visualization, F.L.R.; supervision, F.L.R. and A.D.; project administration, F.L.R. and A.D.; funding acquisition, L.F.A.B. and A.D. All authors have read and agreed to the published version of the manuscript.

Funding: This research received no external funding.

Data Availability Statement: Not applicable.

Acknowledgments: The financial support of Kerbala University and University of Warith Al-Anbiyaa Universities in Iraq is gratefully acknowledged.

Conflicts of Interest: The authors declare no conflict of interest.

Abbreviations

PCMs	Phase change materials
CTES	Cold thermal energy storage
TES	Thermal energy storage
AC	Air conditioning
SEM	Scanning electronic microscopy
DSC	Differential scanning calorimetry
MCNTs	Multiwall carbon nanotubes
FT-IR	Fourier Transform Infrared spectroscopy
HTF	Heat transfer fluid
NCPCMs	Nanocomposite phase change materials
PBTES	Packed bed thermal energy storage
LAES	Liquid air energy storage
LHTES	Latent heat thermal energy storage
GHX	Ground heat exchanger
ANSYS	Analytical system

References

1. BP p.l.c. (Formerly The British Petroleum Company p.l.c and BP Amoco p.l.c). BP statistical review of world energy. *Br. Petrol.* **2010**.
2. Stritih, U.; Charvat, P.; Koželj, R.; Klimes, L.; Osterman, E.; Ostry, M.; Butala, V. PCM thermal energy storage in solar heating of ventilation air—Experimental and numerical investigations. *Sustain. Cities Soc.* **2018**, *37*, 104–115. [CrossRef]
3. Nkwetta, D.N.; Vouillamoz, P.-E.; Haghighat, F.; El Mankibi, M.; Moreau, A.; Desai, K. Phase change materials in hot water tank for shifting peak power demand. *Sol. Energy* **2014**, *107*, 628–635. [CrossRef]
4. Li, G.; Qian, S.; Lee, H.; Hwang, Y. Radermacher, Experimental investigation of energy and exergy performance of short term adsorption heat storage for residential application. *Energy* **2014**, *65*, 675–691. [CrossRef]
5. Li, G.; Hwang, Y.; Radermacher, R. Experimental investigation on energy and exergy performance of adsorption cold storage for space cooling application. *Int. J. Refrig.* **2014**, *44*, 23–35. [CrossRef]
6. Zhang, N.; Yuan, Y.; Cao, X.; Du, Y.; Zhang, Z.; Gui, Y. Latent Heat Thermal Energy Storage Systems with Solid-Liquid Phase Change Materials: A Review. *Adv. Eng. Mater.* **2018**, *20*, 1700753. [CrossRef]
7. Li, G. Energy and exergy performance assessments for latent heat thermal energy storage systems. *Renew. Sustain. Energy Rev.* **2015**, *51*, 926–954. [CrossRef]
8. Qiu, X.; Song, G.; Chu, X.; Li, X.; Tang, G. Microencapsulated n-alkane with p(n-butyl methacrylate-co-methacrylic acid) shell as phase change materials for thermal energy storage. *Sol. Energy* **2013**, *91*, 212–220. [CrossRef]
9. Krupa, I.; Nógellová, Z.; Špitalský, Z.; Malíková, M.; Sobolčiak, P.; Abdelrazeq, H.W.; Ouederni, M.; Karkri, M.; Janigová, I.; Al-Maadeed, M.A.S. Positive influence of expanded graphite on the physical behavior of phase change materials based on linear low-density polyethylene and paraffin wax. *Thermochim. Acta* **2015**, *614*, 218–225. [CrossRef]
10. Qiu, X.; Lu, L.; Han, P.; Tang, G.; Song, G. Fabrication, thermal property and thermal reliability of microencapsulated paraffin with ethyl methacrylate-based copolymer shell. *J. Therm. Anal. Calorim.* **2016**, *124*, 1291–1299. [CrossRef]
11. Puertas, A.M.; Romero-Cano, M.S.; Nieves, F.J.D.L.; Rosiek, S.; Batlles, F.J. Simulations of Melting of Encapsulated CaCl2·6H2O for Thermal Energy Storage Technologies. *Energies* **2017**, *10*, 568. [CrossRef]

12. Smaisim, G.F.; Abed, A.M.; Hadrawi, S.K.; Shamel, A. Modeling and Thermodynamic Analysis of Solar Collector Cogeneration for Residential Building Energy Supply. *J. Eng.* **2022**, *2022*, 6280334. [CrossRef]
13. Stritih, U.; Osterman, E.; Evliya, H.; Butala, V.; Paksoy, H. Exploiting solar energy potential through thermal energy storage in Slovenia and Turkey. *Renew. Sustain. Energy Rev.* **2013**, *25*, 442–461. [CrossRef]
14. Smaisim, G.F.; Al-Madhhachi, H.; Abed, A.M. Study the thermal management of Li-ion batteries using looped heat pipes with different nanofluids. *Case Stud. Therm. Eng.* **2022**, *37*, 102227. [CrossRef]
15. Alharbi, K.A.M.; Smaisim, G.F.; Sajadi, S.M.; Fagiry, M.A.; Aybar, H.; Elkhatib, S.E. Numerical study of lozenge, triangular and rectangular arrangements of lithium-ion batteries in their thermal management in a cooled-air cooling system. *J. Energy Storage* **2022**, *52*, 104786. [CrossRef]
16. Li, Z.X.; Al-Rashed, A.A.; Rostamzadeh, M.; Kalbasi, R.; Shahsavar, A.; Afrand, M. Heat transfer reduction in buildings by embedding phase change material in multi-layer walls: Effects of repositioning, thermophysical properties and thickness of PCM. *Energy Convers. Manag.* **2019**, *195*, 43–56. [CrossRef]
17. Tian, M.-W.; Smaisim, G.F.; Yan, S.-R.; Sajadi, S.M.; Mahmoud, M.Z.; Aybar, H.; Abed, A.M. Economic cost and efficiency analysis of a lithium-ion battery pack with the circular and elliptical cavities filled with phase change materials. *J. Energy Storage* **2022**, *52*, 104794. [CrossRef]
18. Wu, W.; Smaisim, G.F.; Sajadi, S.M.; Fagiry, M.A.; Li, Z.; Shamseldin, M.A.; Aybar, H. Impact of phase change material-based heatsinks on lithium-ion battery thermal management: A comprehensive review. *J. Energy Storage* **2022**, *52*, 104874. [CrossRef]
19. Tian, M.-W.; Abed, A.M.; Yan, S.-R.; Sajadi, S.M.; Mahmoud, M.Z.; Aybar, H.; Smaisim, G.F. Economic cost and numerical evaluation of cooling of a cylindrical lithium-ion battery pack using air and phase change materials. *J. Energy Storage* **2022**, *52*, 104925. [CrossRef]
20. Jiang, Y.; Smaisim, G.F.; Mahmoud, M.Z.; Li, Z.; Aybar, H.; Abed, A.M. Simultaneous numerical investigation of the passive use of phase-change materials and the active use of a nanofluid inside a rectangular duct in the thermal management of lithium-ion batteries. *J. Power Sources* **2022**, *541*, 231610. [CrossRef]
21. Hai, T.; Abidi, A.; Wang, L.; Abed, A.M.; Mahmoud, M.Z.; El Din, E.M.T.; Smaisim, G.F. Simulation of solar thermal panel systems with nanofluid flow and PCM for energy consumption management of buildings. *J. Build. Eng.* **2022**, *58*, 104981. [CrossRef]
22. Dhaidan, N.S.; Kokz, S.A.; Rashid, F.L.; Hussein, A.K.; Younis, O.; Al-Mousawi, F.N. Review of solidification of phase change materials dispersed with nanoparticles in different containers. *J. Energy Storage* **2022**, *51*, 104271. [CrossRef]
23. Rashid, F.L.; Hussein, A.K.; Malekshah, E.H.; Abderrahmane, A.; Guedri, K.; Younis, O. Review of Heat Transfer Analysis in Different Cavity Geometries with and without Nanofluids. *Nanomaterials* **2022**, *12*, 2481. [CrossRef] [PubMed]
24. Rai, U.; Pandey, P. Solidification and thermal behaviour of binary organic eutectic and monotectic; succinonitrile–pyrene system. *J. Cryst. Growth* **2003**, *249*, 301–308. [CrossRef]
25. Baskin, D.G. Fixation and Tissue Processing in Immunohistochemistry. In *Pathobiology of Human Disease*; Elsevier: San Diego, CA, USA, 2014; pp. 3797–3806.
26. Nartowska, E.; Styś-Maniara, M.; Kozłowski, K. The Potential Environmental and Social Influence of the Inorganic Salt Hydrates Used as a Phase Change Material for Thermal Energy Storage in Solar Installations. *Int. J. Environ. Res. Public Health* **2023**, *20*, 1331. [CrossRef] [PubMed]
27. Veerakumar, C.; Sreekumar, A. Phase change material based cold thermal energy storage: Materials, techniques and applications—A review. *Int. J. Refrig.* **2016**, *67*, 271–289. [CrossRef]
28. Nie, B.; Palacios, A.; Zou, B.; Liu, J.; Zhang, T.; Li, Y. Review on phase change materials for cold thermal energy storage applications. *Renew. Sustain. Energy Rev.* **2020**, *134*, 110340. [CrossRef]
29. Selvnes, H.; Allouche, Y.; Manescu, R.I.; Hafner, A. Review on cold thermal energy storage applied to refrigeration systems using phase change materials. *Therm. Sci. Eng. Prog.* **2020**, *22*, 100807. [CrossRef]
30. Radouane, N. A Comprehensive Review of Composite Phase Change Materials (cPCMs) for Thermal Management Applications, Including Manufacturing Processes, Performance, and Applications. *Energies* **2022**, *15*, 8271. [CrossRef]
31. Oró, E.; de Gracia, A.; Castell, A.; Farid, M.M.; Cabeza, L.F. Review on phase change materials (PCMs) for cold thermal energy storage applications. *Appl. Energy* **2012**, *99*, 513–533. [CrossRef]
32. Khan, M.I.; Asfand, F.; Al-Ghamdi, S.G. Progress in research and development of phase change materials for thermal energy storage in concentrated solar power. *Appl. Therm. Eng.* **2023**, *219*, 119546. [CrossRef]
33. Mohamed, S.A.; Al-Sulaiman, F.A.; Ibrahim, N.I.; Zahir, H.; Al-Ahmed, A.; Saidur, R.; Yılbaş, B.S.; Sahin, A.Z. A review on current status and challenges of inorganic phase change materials for thermal energy storage systems. *Renew. Sustain. Energy Rev.* **2016**, *70*, 1072–1089. [CrossRef]
34. Rathod, M.K.; Banerjee, J. Thermal stability of phase change materials used in latent heat energy storage systems: A review. *Renew. Sustain. Energy Rev.* **2013**, *18*, 246–258. [CrossRef]
35. Du, K.; Calautit, J.; Wang, Z.; Wu, Y.; Liu, H. A review of the applications of phase change materials in cooling, heating and power generation in different temperature ranges. *Appl. Energy* **2018**, *220*, 242–273. [CrossRef]
36. Comodi, G.; Carducci, F.; Nagarajan, B.; Romagnoli, A. Application of cold thermal energy storage (CTES) for building demand management in hot climates. *Appl. Therm. Eng.* **2016**, *103*, 1186–1195. [CrossRef]
37. Zou, T.; Fu, W.; Liang, X.; Wang, S.; Gao, X.; Zhang, Z.; Fang, Y. Preparation and performance of form-stable TBAB hydrate/SiO2 composite PCM for cold energy storage. *Int. J. Refrig.* **2019**, *101*, 117–124. [CrossRef]

38. Philip, N.; Dheep, G.R.; Sreekumar, A. Cold thermal energy storage with lauryl alcohol and cetyl alcohol eutectic mixture: Thermophysical studies and experimental investigation. *J. Energy Storage* **2020**, *27*, 101060. [CrossRef]
39. Jebasingh, B.E.; Arasu, A.V. Characterisation and stability analysis of eutectic fatty acid as a low cost cold energy storage phase change material. *J. Energy Storage* **2020**, *31*, 101708. [CrossRef]
40. Alkhwildi, A.; Elhashmi, R.; Chiasson, A. Parametric modeling and simulation of Low temperature energy storage for cold-climate multi-family residences using a geothermal heat pump system with integrated phase change material storage tank. *Geothermics* **2020**, *86*, 101864. [CrossRef]
41. Yang, Y.; Wu, W.; Fu, S.; Zhang, H. Study of a novel ceramsite-based shape-stabilized composite phase change material (PCM) for energy conservation in buildings. *Constr. Build. Mater.* **2020**, *246*, 118479. [CrossRef]
42. Wang, T.; Zhou, X.; Liu, Z.; Wang, J.; Zhang, Y.; Pan, W.-P. Preparation of energy storage materials working at 20–25 °C as a cold source for long-term stable operation. *Appl. Therm. Eng.* **2020**, *183*, 116220. [CrossRef]
43. Dong, X.; Gao, G.; Zhao, X.; Qiu, Z.; Li, C.; Zhang, J.; Zheng, P. Investigation on heat transfer and phase transition in phase change material (PCM) balls and cold energy storage tank. *J. Energy Storage* **2022**, *50*, 104695. [CrossRef]
44. Zheng, L.; Zhang, W.; Liang, F. A review about phase change material cold storage system applied to solar-powered air-conditioning system. *Adv. Mech. Eng.* **2017**, *9*, 1687814017705844. [CrossRef]
45. Jiang, J.-F.; Li, S.-F.; Liu, Z.-H. Study on heat transfer and cold storage characteristics of a falling film type of cold energy regenerator with PCM. *Appl. Therm. Eng.* **2018**, *143*, 676–687. [CrossRef]
46. Said, M.; Hassan, H. Parametric study on the effect of using cold thermal storage energy of phase change material on the performance of air-conditioning unit. *Appl. Energy* **2018**, *230*, 1380–1402. [CrossRef]
47. Sunxi, Z.; Xuelai, Z.; Sheng, L.; Yuyang, L.; Xiaofeng, X. Performance study on expand graphite/organic composite phase change material for cold thermal energy storage. *Energy Procedia* **2019**, *158*, 5305–5310. [CrossRef]
48. Xie, N.; Li, Z.; Gao, X.; Fang, Y.; Zhang, Z. Preparation and performance of modified expanded graphite/eutectic salt composite phase change cold storage material. *Int. J. Refrig.* **2020**, *110*, 178–186. [CrossRef]
49. Karthikeyan, K.; Mariappan, V.; Anish, R.; Sarafoji, P.; Reddy, M.J.B. Experimental study on the charging and discharging behaviour of capric–lauric acid/oleic acid mixture in a cold thermal energy storage system for cold storage applications. *Mater. Today Proc.* **2021**, *46*, 10022–10029. [CrossRef]
50. Ghodrati, A.; Zahedi, R.; Ahmadi, A. Analysis of cold thermal energy storage using phase change materials in freezers. *J. Energy Storage* **2022**, *51*, 104433. [CrossRef]
51. Selvnes, H.; Allouche, Y.; Hafner, A.; Schlemminger, C.; Tolstorebrov, I. Cold thermal energy storage for industrial CO_2 refrigeration systems using phase change material: An experimental study. *Appl. Therm. Eng.* **2022**, *212*, 118543. [CrossRef]
52. Zheng, H.; Tian, G.; Zhao, Y.; Xin, X.; Yang, C.; Cao, L.; Ma, Y. Experimental study on the preparation and cool storage performance of a phase change micro-capsule cold storage material. *Energy Build.* **2022**, *262*, 111999. [CrossRef]
53. Liu, Z.; Lou, F.; Qi, X.; Wang, Q.; Zhao, B.; Yan, J.; Shen, Y. Experimental study on cold storage phase-change materials and quick-freezing plate in household refrigerators. *J. Food Process. Eng.* **2019**, *42*, e13279. [CrossRef]
54. Tas, C.E.; Unal, H. Thermally buffering polyethylene/halloysite/phase change material nanocomposite packaging films for cold storage of foods. *J. Food Eng.* **2020**, *292*, 110351. [CrossRef]
55. Zhan, D.; Zhao, L.; Yu, Q.; Zhang, Y.; Wang, Y.; Li, G.; Lu, G.; Zhan, D.; Li, M. Phase change material for the cold storage of perishable products: From material preparation to material evaluation. *J. Mol. Liq.* **2021**, *342*, 117455. [CrossRef]
56. Du, J.; Nie, B.; Zhang, Y.; Du, Z.; Wang, L.; Ding, Y. Cooling performance of a thermal energy storage-based portable box for cold chain applications. *J. Energy Storage* **2020**, *28*, 101238. [CrossRef]
57. Song, Y.; Zhang, N.; Jing, Y.; Cao, X.; Yuan, Y.; Haghighat, F. Experimental and numerical investigation on dodecane/expanded graphite shape-stabilized phase change material for cold energy storage. *Energy* **2019**, *189*, 116175. [CrossRef]
58. Xiaofeng, X.; Xuelai, Z. Simulation and experimental investigation of a multi-temperature insulation box with phase change materials for cold storage. *J. Food Eng.* **2020**, *292*, 110286. [CrossRef]
59. Liu, K.; He, Z.; Lin, P.; Zhao, X.; Chen, Q.; Su, H.; Luo, Y.; Wu, H.; Sheng, X.; Chen, Y. Highly-efficient cold energy storage enabled by brine phase change material gels towards smart cold chain logistics. *J. Energy Storage* **2022**, *52*, 104828. [CrossRef]
60. Ma, K.; Zhang, X.; Ji, J.; Han, L. Development, characterization and modification of mannitol-water based nanocomposite phase change materials for cold storage. Colloids Surfaces A: Physicochem. *Eng. Asp.* **2022**, *650*, 129571. [CrossRef]
61. Lin, N.; Li, C.; Zhang, D.; Li, Y.; Chen, J. Emerging phase change cold storage materials derived from sodium sulfate decahydrate. *Energy* **2022**, *245*, 123294. [CrossRef]
62. Chang, Y.; Sun, Z. Synthesis and thermal properties of n-tetradecane phase change microcapsules for cold storage. *J. Energy Storage* **2022**, *52*, 104959. [CrossRef]
63. Ikutegbe, C.A.; Al-Shannaq, R.; Farid, M.M. Microencapsulation of low melting phase change materials for cold storage applications. *Appl. Energy* **2022**, *321*, 119347. [CrossRef]
64. Afsharpanah, F.; Pakzad, K.; Ajarostaghi, S.S.M.; Arıcı, M. Assessment of the charging performance in a cold thermal energy storage container with two rows of serpentine tubes and extended surfaces. *J. Energy Storage* **2022**, *51*, 104464. [CrossRef]
65. Browne, M.C.; Norton, B.; McCormack, S.J. Heat retention of a photovoltaic/thermal collector with PCM. *Sol. Energy* **2016**, *133*, 533–548. [CrossRef]

66. Hussain, S.I.; Dinesh, R.; Roseline, A.A.; Dhivya, S.; Kalaiselvam, S. Enhanced thermal performance and study the influence of sub cooling on activated carbon dispersed eutectic PCM for cold storage applications. *Energy Build.* **2017**, *143*, 17–24. [CrossRef]
67. Sze, J.Y.; Mu, C.; Romagnoli, A.; Li, Y. Non-eutectic Phase Change Materials for Cold Thermal Energy Storage. *Energy Procedia* **2017**, *143*, 656–661. [CrossRef]
68. Yu, C.; Yang, S.H.; Pak, S.Y.; Youn, J.R.; Song, Y.S. Graphene embedded form stable phase change materials for drawing the thermo-electric energy harvesting. *Energy Convers. Manag.* **2018**, *169*, 88–96. [CrossRef]
69. Huang, Y.; She, X.; Li, C.; Li, Y.; Ding, Y. Evaluation of thermal performance in cold storage applications using EG-water based nano-composite PCMs. *Energy Procedia* **2019**, *158*, 4840–4845. [CrossRef]
70. Talukdar, S.; Afroz, H.M.M.; Hossain, A.; Aziz, M.; Hossain, M. Heat transfer enhancement of charging and discharging of phase change materials and size optimization of a latent thermal energy storage system for solar cold storage application. *J. Energy Storage* **2019**, *24*, 100797. [CrossRef]
71. Dhivya, S.; Hussain, S.I.; Sheela, S.J.; Kalaiselvam, S. Experimental study on microcapsules of Ag doped ZnO nanomaterials enhanced Oleic-Myristic acid eutectic PCM for thermal energy storage. *Thermochim. Acta* **2019**, *671*, 70–82. [CrossRef]
72. Zou, T.; Liang, X.; Wang, S.; Gao, X.; Zhang, Z.; Fang, Y. Effect of expanded graphite size on performances of modified $CaCl_2 \cdot 6H_2O$ phase change material for cold energy storage. *Microporous Mesoporous Mater.* **2020**, *305*, 110403. [CrossRef]
73. Borri, E.; Sze, J.Y.; Tafone, A.; Romagnoli, A.; Li, Y.; Comodi, G. Experimental and numerical characterization of sub-zero phase change materials for cold thermal energy storage. *Appl. Energy* **2020**, *275*, 115131. [CrossRef]
74. Rakkappan, S.R.; Sivan, S.; Naarendharan, M.; Sudhir, P.S.; Preetham, D.S. Experimental Investigation on Enhanced Energy Storage Characteristics of Spherically Encapsulated 1-Decanol/Expanded Graphite Composite for Cold Storage System. *J. Energy Storage* **2021**, *41*, 102941. [CrossRef]
75. Nie, B.; Chen, J.; Du, Z.; Li, Y.; Zhang, T.; Cong, L.; Zou, B.; Ding, Y. Thermal performance enhancement of a phase change material (PCM) based portable box for cold chain applications. *J. Energy Storage* **2021**, *40*, 102707. [CrossRef]
76. Tafone, A.; Borri, E.; Cabeza, L.F.; Romagnoli, A. Innovative cryogenic Phase Change Material (PCM) based cold thermal energy storage for Liquid Air Energy Storage (LAES)—Numerical dynamic modelling and experimental study of a packed bed unit. *Appl. Energy* **2021**, *301*, 117417. [CrossRef]
77. Rezaei, H.; Ghomsheh, M.J.; Kowsary, F.; Ahmadi, P. Performance assessment of a range-extended electric vehicle under real driving conditions using novel PCM-based HVAC system. *Sustain. Energy Technol. Assessments* **2021**, *47*, 101527. [CrossRef]
78. Sarafoji, P.; Mariappan, V.; Anish, R.; Karthikeyan, K.; Kalidoss, P. Characterization and thermal properties of Lauryl alcohol—Capric acid with CuO and TiO_2 nanoparticles as phase change material for cold storage system. *Mater. Lett.* **2022**, *316*, 132052. [CrossRef]
79. Wang, F.; Xia, X.; Lv, Y.; Cheng, C.; Yang, L.; Zhang, L.; Zhao, J. Heat transfer, energy conversion, and efficiency during cold discharge of a novel tetrabutylammonium bromide hydrate cold storage system. *Appl. Therm. Eng.* **2022**, *211*, 118462. [CrossRef]
80. Mousavi, S.B.; Ahmadi, P.; Hanafizadeh, P.; Khanmohammadi, S. Dynamic simulation and techno-economic analysis of liquid air energy storage with cascade phase change materials as a cold storage system. *J. Energy Storage* **2022**, *50*, 104179. [CrossRef]
81. Wu, J.; Chen, Q.; Zhang, Y.; Sun, K. A novel design of discrete heat and cold sources for improving the thermal performance of latent heat thermal energy storage unit. *J. Energy Storage* **2022**, *50*, 104199. [CrossRef]
82. Laouer, A.; Teggar, M.; Tunçbilek, E.; Arıcı, M.; Hachani, L.; Ismail, K.A. Melting of hybrid nano-enhanced phase change material in an inclined finned rectangular cavity for cold energy storage. *J. Energy Storage* **2022**, *50*, 104185. [CrossRef]
83. Feng, J.; Ling, Z.; Huang, J.; Fang, X.; Zhang, Z. Experimental research and numerical simulation of the thermal performance of a tube-fin cold energy storage unit using water/modified expanded graphite as the phase change material. *Energy Storage Sav.* **2022**, *1*, 71–79. [CrossRef]
84. Liu, G.; Li, Q.; Wu, J.; Xie, R.; Zou, Y.; Marson, A.; Scipioni, A.; Manzardo, A. Improving system performance of the refrigeration unit using phase change material (PCM) for transport refrigerated vehicles: An experimental investigation in South China. *J. Energy Storage* **2022**, *51*, 104435. [CrossRef]
85. Singh, P.; Sharma, R.; Ansu, A.; Goyal, R.; Sarı, A.; Tyagi, V. A comprehensive review on development of eutectic organic phase change materials and their composites for low and medium range thermal energy storage applications. *Sol. Energy Mater. Sol. Cells* **2021**, *223*, 110955. [CrossRef]